

# Radiation-Hardened Electronics for Reactor Environments



**Approved for public release.  
Distribution is unlimited.**

F. Kyle Reed  
N. Dianne Bull Ezell  
M. Nance Ericson  
Charles L. Britton, Jr.

**October 2020**

#### DOCUMENT AVAILABILITY

Reports produced after January 1, 1996, are generally available free via US Department of Energy (DOE) SciTech Connect.

**Website:** <http://www.osti.gov>

Reports produced before January 1, 1996, may be purchased by members of the public from the following source:

National Technical Information Service  
5285 Port Royal Road  
Springfield, VA 22161  
**Telephone:** 703-605-6000 (1-800-553-6847)  
**TDD:** 703-487-4639  
**Fax:** 703-605-6900  
**E-mail:** [info@ntis.gov](mailto:info@ntis.gov)  
**Website:** <http://classic.ntis.gov/>

Reports are available to DOE employees, DOE contractors, Energy Technology Data Exchange representatives, and International Nuclear Information System representatives from the following source:

Office of Scientific and Technical Information  
PO Box 62  
Oak Ridge, TN 37831  
**Telephone:** 865-576-8401  
**Fax:** 865-576-5728  
**E-mail:** [report@osti.gov](mailto:report@osti.gov)  
**Website:** <http://www.osti.gov/contact.html>

This report was prepared as an account of work sponsored by an agency of the United States Government. Neither the United States Government nor any agency thereof, nor any of their employees, makes any warranty, express or implied, or assumes any legal liability or responsibility for the accuracy, completeness, or usefulness of any information, apparatus, product, or process disclosed, or represents that its use would not infringe privately owned rights. Reference herein to any specific commercial product, process, or service by trade name, trademark, manufacturer, or otherwise, does not necessarily constitute or imply its endorsement, recommendation, or favoring by the United States Government or any agency thereof. The views and opinions of authors expressed herein do not necessarily state or reflect those of the United States Government or any agency thereof.

Electrification and Energy Infrastructure Division  
Nuclear Energy and Fuel Cycle Division

**Radiation-Hardened Electronics for Reactor Environments**

F. Kyle Reed  
N. Dianne Bull Ezell  
M. Nance Ericson  
Charles L. Britton, Jr.

Date Published: October 2020

Prepared by  
OAK RIDGE NATIONAL LABORATORY  
Oak Ridge, TN 37831-6283  
managed by  
UT-Battelle, LLC  
for the  
US DEPARTMENT OF ENERGY  
under contract DE-AC05-00OR22725



# CONTENTS

LIST OF FIGURES . . . . .	v
LIST OF TABLES . . . . .	vii
ACRONYMS . . . . .	ix
ABSTRACT . . . . .	1
1. INTRODUCTION . . . . .	1
1.1 RADIATION-HARDENED ELECTRONICS FOR SPACE APPLICATIONS . . . . .	1
1.2 RADIATION AND TEMPERATURE ENVIRONMENTS FOR NUCLEAR APPLICATIONS . . . . .	2
1.3 RADIATION EFFECTS ON ELECTRONIC COMPONENTS . . . . .	4
1.3.1 Neutron Effects: Displacement Damage . . . . .	5
1.3.2 Gamma Effects: TID and Dose Rate . . . . .	5
2. CURRENT STATE-OF-THE-ART RADIATION-HARDENED ELECTRONICS . . . . .	6
2.1 PASSIVE DEVICES . . . . .	7
2.1.1 Capacitors . . . . .	7
2.1.2 Cables and Interconnects . . . . .	8
2.1.3 Inductors and Printed Circuit Boards . . . . .	10
2.2 DISCRETE ACTIVE DEVICES . . . . .	11
2.2.1 Diodes, LEDs, and Photodiodes . . . . .	12
2.2.2 Bipolar Junction Transistors . . . . .	14
2.2.3 Metal-Oxide-Semiconductor Field Effect Transistors . . . . .	15
2.2.4 Complementary Metal-Oxide-Semiconductor Technology . . . . .	17
2.2.5 Junction Field Effect Transistors . . . . .	18
2.2.6 Wide Bandgap Devices . . . . .	19
2.2.7 Vacuum Devices . . . . .	19
2.3 INTEGRATED CIRCUITS . . . . .	20
2.3.1 Voltage Regulators and Power Devices . . . . .	20
2.3.2 Operational Amplifiers . . . . .	21
2.3.3 Analog and Digital Converters . . . . .	22
2.3.4 Digital and Mixed Signal Integrated Circuits . . . . .	23
2.3.5 Data-Links and Communication Interfaces . . . . .	24
2.3.6 Commercial IC Offerings . . . . .	25
2.4 SYSTEMS . . . . .	29
2.4.1 Cameras . . . . .	29
2.4.2 Power Conversion and Harvesting Systems . . . . .	29
2.4.3 Communications and Controls . . . . .	29
2.4.4 Robots and Remote Operations . . . . .	30
3. GAPS AND FUTURE DIRECTIONS IN NUCLEAR RADIATION HARDENED ELECTRONICS	30
4. CONCLUDING REMARKS . . . . .	32
5. REFERENCES . . . . .	33



## LIST OF FIGURES

1	Areas of concern for shielding . . . . .	3
2	Maximum operating temperatures of four generations of reactor technologies . . . . .	5
3	Comparison of the radiation sensitivity of various capacitor materials . . . . .	8
4	Comparison of the radiation resistance of cable dielectric materials . . . . .	10
5	Measured RIA of SiO <sub>2</sub> FO cables by Cheymol et al. and Brichard et al. with a radiation-induced compaction model . . . . .	11
6	Cross section of a pn junction diode . . . . .	13
7	Cross section of an NPN BJT . . . . .	15
8	Cross section of an NMOS transistor . . . . .	16
9	CMOS process cross section . . . . .	17
10	Cross section of an pJFET transistor . . . . .	18



## LIST OF TABLES

1	Water reactor technology parameters . . . . .	4
2	Environment conditions for reactors, nuclear weapons, and space . . . . .	4
3	Neutron displacement damage on active device technologies . . . . .	12
4	Gamma TID damage on active device technologies . . . . .	12
5	Commercial space-rated device offerings from STMicroelectronics . . . . .	26
6	Commercial space-rated device offerings from Renesas–Intersil . . . . .	27
7	Commercial space-rated device offerings from BAE Systems . . . . .	27
8	Commercial space-rated device offerings from Xilinx . . . . .	28
9	Commercial space-rated device offerings from Texas Instruments . . . . .	28



## ACRONYMS

AC	alternating current
ADC	analog-to-digital converter
APS	active pixel sensor
ASIC	application-specific integrated circuit
BiCMOS	bipolar CMOS
BJT	bipolar junction transistor
BWR	boiling [light] water reactor
CCD	charge-coupled device
COTS	commercial off the shelf
CMOS	complementary metal oxide semiconductor
CMRR	common mode rejection ratio
CRT	cathode ray tube
DAC	digital-to-analog converter
DC	direct current
DOE	US Department of Energy
EMI	electromagnetic interference
FET	field effect transistor
FO	fiber optic
FPGA	field programmable gate array
GBT	gigabit transceiver
GCR	galactic cosmic ray
GPIB	general purpose integrated bus
IC	integrated circuit
INL	Idaho National Laboratory
ITER	International Thermonuclear Experimental Reactor
FPGA	field programmable gate array
JFET	junction field effect transistor
LED	light emitting diode
LEO	low-earth orbit
LVDS	low voltage differential signaling
LWRS	light-water reactor
MCU	microcontroller unit
MgO	magnesium oxide
MI	mineral insulated
MOSFET	metal oxide semiconductor field effect transistor
NE	Office of Nuclear Energy
NEET	Nuclear Energy Enabling Technologies
NMOS	N-type MOSFET
NPP	nuclear power plant
opamps	operational amplifiers
ORNL	Oak Ridge National Laboratory
PCB	printed circuit board
PCI	peripheral component interconnect
PE	polyethylene

PMOS	p-type MOSFET
PSSR	power supply rejection ratio
PTFE	polytetrafluoroethylene
PWM	pulse-width modulation
PWR	pressurized [light] water reactor
RHA	radiation hardness assurance
RIA	radiation-induced attenuation
RHBD	rad-hard by design
RHBP	rad-hard by process
RF	radio frequency
SCSI	small computer system interface
SCWR	supercritical water-cooled reactor
SEE	single-event effect
SEL	single-event latchup
SERDES	serializer-deserializer
SEU	single-event upset
SiC	silicon-carbide
SIMON	semi-intelligent mobile observing navigator
SNIR	signal-to-noise-plus-interference ratio
SOA	state of the art
SoC	system-on-chip
SPI	serial peripheral interface
SPICE	simulation program with integrated circuit emphasis
TID	total ionizing dose
TMR	triple modular redundancy
TPI	thermoplastic polyimide
TTL	transistor-transistor logic
VLSI	very large-scale integration
WBG	wide-bandgap
WMC	wall-mounted cubicle

## **ABSTRACT**

Radiation-hardened (rad-hard) electronics have been the shortcoming in nuclear sensing and instrumentation. Placing advanced sensors and associated electronics closer to a nuclear reactor core will improve reactor control and operation through increased signal accuracy, precision, and fidelity, resulting in safer, more efficient energy production. However, the extreme temperature and bombarding radiation environment of nuclear applications make research and development into electronics and electronic materials technologies essential to enabling improved safety, monitoring, and control of the existing nuclear reactor fleet and the next generation of reactors, including microreactors. To help the US Department of Energy (DOE) define a course for the Office of Nuclear Energy (NE)-funded rad-hard electronics research, Oak Ridge National Laboratory staff present this summary of the state-of-the-art (SOA) technology for the design and implementation of rad-hard electronics and systems, including research efforts and commercial offerings. A collection of technological gaps associated with reactor applications are compiled herein. Based on the radiation degradation mechanisms discussed in this report, along with the state-of-the-art summary survey and a compiled list of gaps, a high-level research plan of future NE funding direction was developed and is provided. This report outlines these activities and provides a summary of SOA electronics technology for rad-hard instrumentation in reactors, a list of the major technology gaps observed, and a draft plan for addressing the present and future needs of reactor instrumentation.

## **1. INTRODUCTION**

Electronics for radiological applications such as nuclear or space applications lag behind commercially available consumer electronics in terms of computational power, efficiency, and maturity. As the state of the art (SOA) of radiation-hardened (rad-hard) electronics advances and interest develops for near- or in-core nuclear instrumentation within the existing reactor fleet, and as advanced reactor designs become reality, technology gaps with clearly defined research directions are becoming prevalent. Instrumentation using optimally placed rad-hard electronics would improve reactor safety and efficiency by reducing the noise typically injected on the lengthy cabling between the sensor and electronics. Optimally placed rad-hard electronics would increase signal integrity and would allow for the use of fiber optic or wireless signal transmission. The options of available rad-hard electronics for space and satellite systems bombarded with cosmic galactic rays, protons, and electrons is extensive compared to the limited high-temperature, rad-hard electronic devices and systems available for use in the high neutron and gamma environments near or within reactor cores.

To increase the market density of suitable reactor-rated rad-hard electronics, radiation-attributed degradation and the limits of SOA electronic components and systems must be understood. This document details the radiation environments of space and nuclear applications, the effects of radiation degradation mechanisms on electronic components, the SOA in rad-hard electronics that are commercially available, and current research directions. Technological gaps are presented with associated research directions and objectives to cultivate safer, more efficient reactor environments through the incorporation and deployment of rad-hard sensors and electronics systems.

### **1.1 RADIATION-HARDENED ELECTRONICS FOR SPACE APPLICATIONS**

NASA and its satellite industry partners have significantly advanced electronics technologies and commercial options for space applications. However, the radiation environment in space differs from that in a typical

operating nuclear reactor. Galactic cosmic rays (GCRs) are the predominant source of ionizing radiation, and they consist of atomic nuclei with gigaelectron volt (GeV) characteristic energies that are produced by massively energetic events such as supernovas. Solar winds that are emitted from the sun are comprised of protons and electrons with keV-characteristic energy levels [1]. Other transient solar events, such as solar flares or coronal mass ejections, generate protons, x-rays, and heavy atomic nuclei with energies ranging from MeV to tens of MeV.

Earth's magnetic field traps proton, electron, and heavy ion radiation into regions known as the Van Allen Belts through magnetic forces. Trapped particles in the Van Allen Belts create concerns for low-earth orbit (LEO) applications such as satellites or space stations. However, deep space missions are affected by neutrons if a reactor is used for propulsion and power. Single event effects (SEEs) are the prominent concern of satellite applications. Shielding is implemented to protect electronics, but the high energy radiation and mass constraints in spaceflights reduce the effectiveness. Passive shielding is effective for solar particle events but is limited for GCR [2]. To reduce the fuel costs typically incurred by transporting heavy shielding materials into space, existing infrastructure such as water or fuel is widely used. However, the effectiveness of this approach is limited. Ideally, creating a shield from a material with the highest ratio of electrons to nucleon per atom, such as polyethylene and hydrogen-embedded nanofibers, would minimize secondary radiation production to shield from GCR [2].

The four main areas of concern for shielding are (1) shield geometry and shielding analysis technique, (2) shield material composition, (3) component composition (e.g., package, passivation, metalization and semiconductor materials of a complex microcircuit), and (4) dose units. Using the diagram in Figure 1, scientists can determine whenever calculations are performed and shielding is required (including which shielding materials are require for the radiation environment).

Shielding is not the only possible solution for protecting the electronics from excessive radiation exposure. Appropriate mission planning/scheduling to avoid radiation fields can also reduce exposure time. Hardening by architecture uses redundant commercial parts in duplicate architectures to mitigate radiation induced effects. However, this method increases the power consumption, weight, and size. Radiation hardening by design (RHBD) makes use of chip layout techniques, device spacing, decoupling, correction circuits, etc. Radiation hardening by process (RHBP) employs known radiation-tolerant materials and processing techniques, but these materials increase the cost of the electronics. NASA has developed a radiation hardness assurance (RHA) methodology process that includes the following steps: (1) define the radiation hazard, (2) evaluate the hazard, (3) define the requirements to be met by the spacecraft's electronics, (4) evaluate the electronics to be used, (5) engineer processes to mitigate hazard damage, and (6) iterate on the methodology as necessary [4].

## **1.2 RADIATION AND TEMPERATURE ENVIRONMENTS FOR NUCLEAR APPLICATIONS**

The existing fleet of reactors within the United States varies widely in terms of age, location, and reactor type or design. Furthermore, most of the design information is tightly controlled for safety [5]. Over the last 10 years, the US Department of Energy (DOE) Light Water Reactor Sustainability program has been studying structural degradation of concrete, cabling, and other materials to reduce maintenance costs through predictive modeling [6] of the existing reactor fleet. This includes the degradation of instrumentation from high temperature and radiation environments.

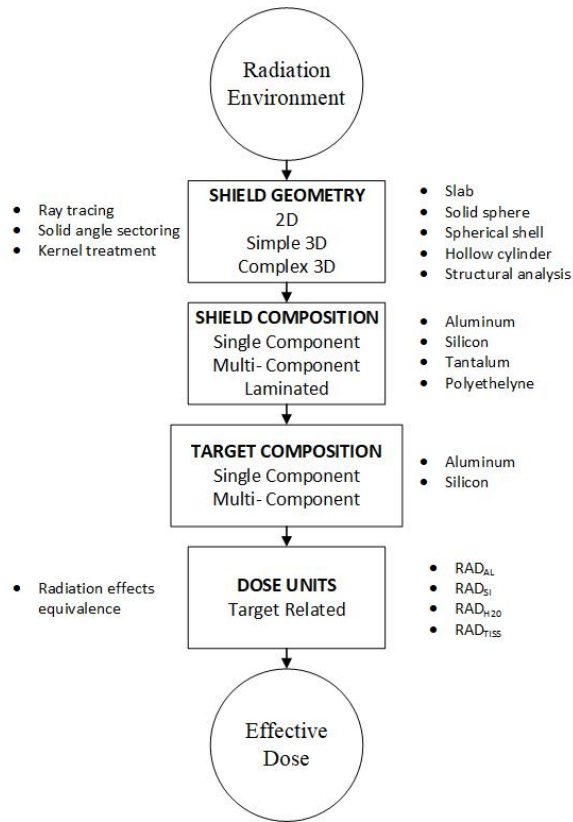


**Figure 1. Areas of concern for shielding [3].**

The radiation and temperature environments within existing fission reactors vary for pressurized light-water reactors (PWRs); boiling light-water reactors (BWRs); gas-cooled reactors; as well as heavy-water, graphite-moderated, and liquid-metal-cooled reactors. This report addresses PWRs and BWRs since they are the most prevalent reactor types in the world’s nuclear fleet. The pressurized water in a ~15.5 MPa PWR enters the core at approximately 275°C and exits the core at 325°C [7]. Similarly, BWR operating temperatures are around 285–300°C. The radiation environment is detailed in Table 1.

While BWRs and PWRs are both light-water reactors (LWRs), BWRs have a single water circuit design which does not require a steam generator or pressurizer. This allows boiling to occur in the core with steam flowing directly to the turbine. A supercritical water-cooled reactor is a Generation 4 reactor designed to operate like a LWR, but at supercritical pressures.

The accumulated radiation doses and fluences in containment for long-term plant operation and space or nuclear weapons storage environments are compared in Table 2 [5]. Since rad-hard electronics are under development for space environment applications, it is important to document these conditions and highlight the lack of studies within nuclear reactor environments.

The next generation of reactors will have greater environmental hazards, such as high operating temperatures to increase thermal efficiency (Figure 2). The increased temperatures limit the survivability of sensor and electronics materials. Also, these reactors take advantage of both fast neutron flux and thermal neutron flux. Each flux type has its own degradation mechanisms. For example, chronic thermal flux exposure causes transmutation through absorption of neutrons.

**Table 1. Table of water reactor technology parameters [7].**

System	Coolant	Pressure (MPa)	Temp <sub>in</sub> /Temp <sub>out</sub> (°C)	Neutron spectrum max dose (dpa)	Fuel type
PWR	Water: single phase	16	290/320	Thermal, ~80	UO <sub>2</sub> (or MOX)
BWR	Water: two phase	7	280/288	Thermal, ~7	UO <sub>2</sub> (or MOX)
Supercritical water-cooled reactor	Supercritical water	25	290/6,000	Thermal, ~30, Fast, ~70	UO <sub>2</sub>

**Table 2. Environment conditions for reactor, nuclear weapons, and space [5].**

Environment	Reactor containment (normal operation, 40 yr)	Nuclear weapons stockpile (20–25 yr)	Space (5-year mission)
Gamma <sup>a</sup> rad(Si) [rad(Si)/hr]	10 <sup>3</sup> -10 <sup>8</sup> [10 <sup>3</sup> -10 <sup>8</sup> ]	5×10 <sup>3</sup>	-
Neutron <sup>b</sup> n/cm <sup>2</sup> [n/cm <sup>2</sup> sec]	10 <sup>9</sup> -10 <sup>14</sup> [10 <sup>0</sup> -10 <sup>5</sup> ]	-	-
Electron/proton rad(Si) [rad(Si)/hr]	-	-	10 <sup>5</sup> -10 <sup>6</sup> [3]

<sup>a</sup> Gamma dose: Nuclear plant containment, <10<sup>8</sup> between primary and secondary shield, <10<sup>6</sup> outside secondary shield.

<sup>b</sup> Neutron energies: Nuclear plant containment (outside secondary shield), median energy ~100 keV; Weapons test, >10 keV. The same dose deposited in silicon from 1 MeV neutrons would reduce the flux and fluence numbers for 100 keV neutrons by a factor of 10–20.

### 1.3 RADIATION EFFECTS ON ELECTRONIC COMPONENTS

As discussed in Section 1.2, neutron and gamma radiation are the primary sources of radiological activity in nuclear power plants (NPPs) and other nuclear environments. Both of these sources have deleterious effects on electronic systems and their associated components. This section provides a discussion of the implications of radiation effects on electronics. Information on the effects of these radiations on a particular device or system can be found in its respective section.

The effects of radiation in electronic systems can be divided into three broad categories: displacement damage, total ionizing dose (TID) effects, and dose-rate effects. *Displacement damage* occurs when a particle displaces an atom in a semiconductor lattice upon collision, which disrupts the local lattice structure. *TID* degradation manifests most commonly as charge trapping, electric and magnetic field generation, and chemical effects. *Dose-rate effects* manifest commonly as transient disruptions changing the state of the device. These events occur when a single particle collision transfers sufficient energy to cause non-damaging single-event upsets (SEUs) or damaging events such as single-event latchups (SELs). Displacement damage and TID are both considered cumulative, long-term effects, while dose-rate effects may be considered short term or temporary in many applications.

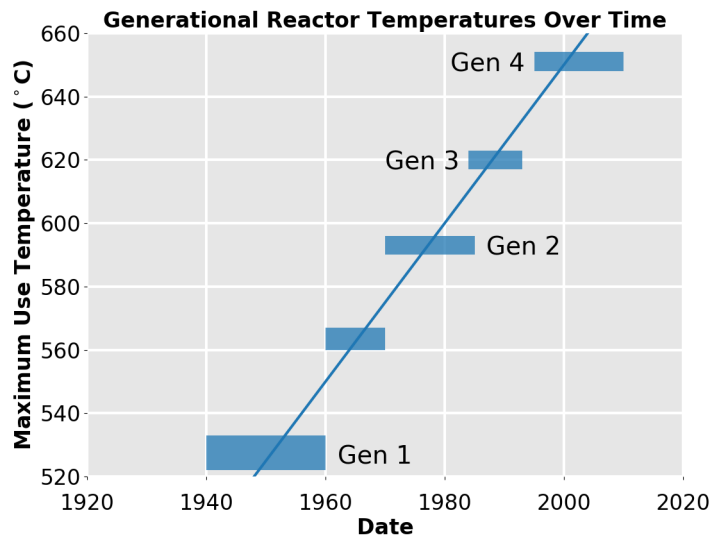


**Figure 2. Historical observation of maximum operating temperature for four generations of reactor technologies based on results summarized by Viswanathan [8].**

### 1.3.1 Neutron Effects: Displacement Damage

Displacement damage occurs when heavy particles such as neutrons displace atoms from their lattice structure upon collision. This is a form of nonionizing damage and is commonly expressed in units of atoms/cross section. Neutron fluence is defined as the number of neutrons of energy  $E$  per  $\text{cm}^2$  ( $\text{n}/\text{cm}^2$ ) penetrating a medium, and flux is defined as the number of neutrons of energy  $E$  per cross sectional area per unit time ( $\text{n}/\text{cm}^2$ ). These are the principle quantities used to discuss these effects.

Displacement damage depends on the kinematics of the displacement particle. High-energy (fast) neutrons will transfer their energy to interstitial atoms, which can cause cascaded displacements. Displaced atoms may recombine with dopant or impure atoms into vacancies, thus producing stable defect sites. These sites form trapping centers that result in increased material resistivity and electronic noise.

Annealing, or self-healing, of displacement defects can occur at room temperature due to the inherent instability of displaced atoms. However, this recombination may associate with impurities in the lattice structure instead of in the lattice itself, resulting in the formation of new trapping centers.

### 1.3.2 Gamma Effects: TID and Dose Rate

Photons of high energy (gamma) may interact with atoms by the Compton effect, releasing a valence electron from the outer shell by collision. If the gamma ray has higher energy, then a phenomenon occurs in which the electron is annihilated spontaneously when near the atomic nucleus. A fast-moving positron and electron appear in place of the photon, conserving the neutral charge of the photon. This is referred to as *pair creation*, and both particles contribute to ionizing radiation. Ionizing radiation can be classified as resulting from either TID or flux-rate effects. Long-term TID effects are related to charge-trapping and chemical effects, whereas short-term flux-rate effects produce increased photocurrents, propagation delays, and SEEs

such as SEUs and SELs.

Charge-trapping in materials due to gamma dose occurs most readily in electrical insulators (materials with resistivity greater than  $10^5 \Omega \cdot m$ ) due to their low electron mobility. When an insulator is subject to high-energy photons (gamma or x-ray), injected electrons, or those resulting from ionization, trapped components of these charges accumulate. Electric fields between insulating materials and nearby conductors are generated from opposing neutralizing charges. If the electric field increases beyond the conductivity, then electrical breakdown occurs. Induced space charge may linger for days in insulators. Induced charges may alter the permanent chemical composition of materials if the charges are sufficient to rupture covalent chemical bonds, atomic bonds formed between atoms via shared electron pairs.

In semiconductors, the electron-hole pairs formed from ionization occur within the oxide layers. For silicon, the specific ionization density is about  $4.2 \times 10^{13}$  electron-hole pairs/( $\text{cm}^3 \cdot \text{rad}$  (Si)) and is temperature independent [9]. Even if the produced electron or hole lacks the energy to span the material band gap, it may still reach the edge of the gap and become trapped. This is similar to the operating principle of doped infrared detectors. If the released electrons are swept or leaked from the material, then an electric field will be produced, resulting in a drift current.

Uniformly distributed electron-hole pairs from homogeneous and isotropic transient ionizing radiation incident on a semiconductor are created. The charge carriers formed near the boundary region of the pn-junction, a junction between p-doped and n-doped regions of semiconductor materials, will cross due to drift creating photocurrents. A photocurrent is an electric current through a photosensitive medium like a pn-junction. Electron-hole pairs are generated proportionally to the incident radiation flux, depending on the total energy absorbed by the material of interest. At high incident pulse radiation intensities, these photocurrents can manifest as noisy signals, or they can be magnitudes greater than the signal levels. These increase linearly with dose rates up to approximately 1 MGy/s, whereas the photocurrent increases at a greater rate until it reaches device saturation. The device may remain saturated for a period of time, even after the dose rate drops. The dose rate also increases propagation delays in the signal by remaining saturated for prolonged intervals.

SEEs occur as an erroneous bit in logic circuits when no degradation is exhibited, and they occur through ionization processes. As semiconductor density in very large-scale integrated (VLSI) circuits has increased as described by Moore's law, vulnerability to SEEs has increased. The smaller feature sizes and lower switching voltages required for increased semiconductor density reduce the incident dose rate and energy required to produce a bit error. Triple modular redundancy (TMR), in which three systems perform a calculation or task simultaneously with a majority-voting system, is a common SEE mitigation strategy for digital circuits. In electronic memory, error correction codes have also been used to preserve data using bit redundancy, requiring additional memory space proportionally smaller than the tripling of hardware structures associated with TMR techniques.

## **2. CURRENT STATE-OF-THE-ART RADIATION-HARDENED ELECTRONICS**

Electronics deployed in nuclear reactor and fuel storage environments can increase safety and reliability by measuring and relaying accurate conditions to control systems and operators, implementing real-time control operations, and increasing computational power. As SOA electronics advance, their environment associated failure mechanisms and computation limits need to be better understood to improve modern reactor systems

and to be integrated into emerging advanced reactor technologies. This section outlines electronic device limitations, starting with the basic passive components inherent in every electronics system, active devices, integrated circuits, and full electronics systems.

## 2.1 PASSIVE DEVICES

Passive devices are found in every electronics system. Although the major limiting factor of electronic systems is predominantly active devices, passive devices also exhibit temporary and permanent fluctuations and degradation. As a general rule of thumb, components based on organic materials are much more susceptible to radiation effects than inorganic alternatives. However, all device types can experience minor degradation or variations in component properties. Variations in component properties are dependent on the radiation dose or dose rate, and they may require application-specific in situ compensation or re-calibration procedures.

### 2.1.1 Capacitors

Capacitors are passive electrical components that store energy in the form of an electric field. They are composed of electrodes separated by a dielectric substrate in varying geometries. In electronic circuits, capacitors are often used as filters for AC coupling (DC-block) or decoupling. They serve a critical function in integrated circuits, as they are commonly used to maintain a consistent DC voltage (buffered against rapid transients) on the power rails.

Many different dielectric materials are used for capacitors, depending on the specifics of the application or use. Common materials employed for capacitor dielectrics include ceramics, glass, mica, paper, plastic films, and oxides. These dielectric materials, along with the geometries used to fabricate a capacitor, dictate its voltage and current limitations. Ceramic, glass, and mica capacitors feature high insulation resistance and low dissipation factors. In contrast, paper and electrolytic (oxide) capacitors have low insulation resistance and high dissipation factors.

Radiation-induced capacitor parameter variations may degrade circuit performance. The main source of capacitor variation during irradiation is the induced dimensional changes of the inter-electrode space [10]. This is most common in capacitors using organic insulators as dielectrics. Gas evolution within these materials under irradiation creates high-pressure regions in the device that distort the capacitor or rupture the device seals.

Capacitors under irradiation will experience temporary effects attributed to the flux rate, as well as permanent changes due to the TID. The temporary capacitive changes due to irradiation are greater in magnitude than the permanent effects. If the flux rates are time-variant, then adequate system compensation may be required to mitigate reduced device performance. Irradiation sensitivity of various capacitors due to fast neutron fluence and TID are compared in Figure 3.

Inorganic capacitors such as ceramic, glass, and mica are the preferred capacitor types for rad-hard electronics design. Ceramic capacitors generally experience decreasing capacitance during irradiation. The typical maximum capacitance change of ceramic capacitors is in the range of 10–15% [10]. Some of the capacitance variation of ceramics may be attributed to temperature variations. Glass-dielectric capacitors have shown a maximum temporary variation in capacitance of 4.0% and permanent variations in capacitance of 3.1% in radiation environments between  $5.7 \times 10^{16}$  n/cm<sup>2</sup> and  $3.4 \times 10^{18}$  n/cm<sup>2</sup> neutron fluence and gamma TID of

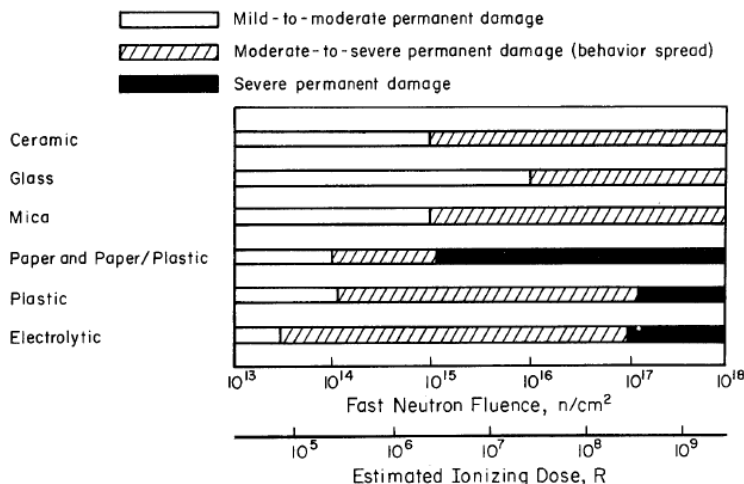


**Figure 3. Comparison of the radiation sensitivity of various capacitor materials [10].**

7.7 and 30 MGy (C) [10]. Mica capacitance measurements have been shown to have permanent changes of up to 6.0% for neutron fluences of  $6 \times 10^{15}$  n/cm<sup>2</sup> and gamma doses up to 1 MGy (C) [10].

Film-dielectric capacitors are two to three orders of magnitude more sensitive to radiation than the aforementioned inorganic capacitors due to their oil impregnation releasing hydrogen or hydrocarbon gases. The gaseous release increases the pressure buildup, thus deforming the capacitor structure. As capacitance is dependent on the inter-electrode spacing and area in conjunction with the dielectric constant of materials, structural changes in these parameters will affect the device capacitance and dissipation factor. Variations of capacitance up to 50% have been recorded for film capacitors [10].

Electrolytic and tantalum capacitors use an oxide layer over the electrodes to form the dielectric electrode stack. The closer plate geometries created by the thin oxide layers enable these capacitors to have a greater capacitance-to-volume ratio than the aforementioned capacitors. However, electrolytic capacitors are more susceptible to increasing leakage as a function of increasing flux rates [9].

Supercapacitors (also referred to as *ultracapacitors*) are an emerging technology that seeks to close the energy density gap between capacitors and batteries. These supercapacitors have an even greater capacitance-to-volume ratio than electrolytic capacitors. These devices have been shown to increase capacitance by as much as 20% during irradiation of  $4.05 \times 10^{14}$  n/cm<sup>2</sup> thermal neutrons,  $1.75 \times 10^{13}$  n/cm<sup>2</sup> fast neutrons, and 75 kGy TID of gamma radiation [11]. More recent work suggests that more modern supercapacitors have negligible changes compared to normal aging of the devices [12].

More information on capacitor insulation resistance and dissipation factor variations due to radiation is discussed in greater detail in the work by Hanks and Hammon [10].

### 2.1.2 Cables and Interconnects

Cables and connectors are the primary channel for linking electrical system components. Signals providing sensor or control information are transmitted through cables, requiring adequate shielding against electromagnetic interference (EMI) and noise to preserve signal integrity. Power is delivered through cables that

require an optimized conductor size to prevent large voltage drops over their lengths without inhibiting necessary bending. In a nuclear environment, these cables are likely to be routed through high-radiation zones.

Insulation stability is critical for signal-carrying cables. When a signal is propagated on a conductor length on the order of one thousandth of the signal wavelength, the conductor must be regarded as a transmission line. Transmission lines require impedance matching to maintain signal fidelity, as RF effects such as RF radiation, crosstalk, and signal reflections will become more prominent with increasing impedance mismatch. For example, coaxial camera cables are produced to have a 75 ohm characteristic impedance, and many RF circuit impedances match to 50 ohms. The characteristic impedance of a cable is a function of the dielectric constant of the insulation, the insulation resistance, and the geometry of the cable, such as conductor separation. Although the characteristic impedance effects on low-frequency signals and power are negligible, cable failure and leakage currents are still a concern at higher irradiation levels.

Flexible cables are preferred for temporary infrastructures such as those developed for experimentation and testing, or for applications requiring limited movement. Radiation-resistant flexible cables are commercially available, with those made using thermoplastic polyimide (TPI) and polyimide that can withstand 200 MGy and 100 MGy, respectively, in standard atmospheric conditions. These doses increase to >500 MGy for inert atmospheres [13]. An assortment of other materials is shown in Figure 4. It is important to note that the polytetrafluoroethylene (PTFE) used in RG174 BNC cables has a radiation resistance of 1 kGy, and the polyethylene (PE) used in RG58 BNC cables has a radiation resistance of and 100 kGy.

For cases in which installations do not require movement, it is best to use inflexible cables. Among inflexible cable types are the market standard mineral-insulated (MI) cables that have been tested for decades. These cables are fabricated with one or more conductive rods housed within a sheath filled with alumina ( $Al_2O_3$ ), or magnesium oxide (MgO). MI cables insulated with MgO have been shown to survive up to 100 MGy gamma TID and  $10^{18}$  n/cm<sup>2</sup> [14]. As these cables are both radiation and fire rated, they have been successfully used in extreme radiation environments, and even in reactor core applications [15]. Radiation-induced electromotive force effects on MI cables have been known to generate spurious signals on the order of nanoamps or microvolts due to ionizing radiation interactions [14].

Fiber optic (FO) cables are increasingly used in high-speed telecommunications and sensing applications. Irradiation induces defects on fiber optic cables that attenuate an optically transmitted signal. Amorphous-fused silica (a-SiO<sub>2</sub>)-based FO cables have increasing radiation-induced attenuation (RIA) with increasing wavelengths and neutron fluence [16], with the 800–1000 nm range being the least attenuated by neutrons, as shown in Figure 5. Furthermore, 20 dB/m attenuation can be expected for  $3.2 \times 10^{19}$  n/cm<sup>2</sup> at 50°C and 1200 nm. This attenuation is believed to decrease with increasing temperatures.

Silica (SiO<sub>2</sub>) and sapphire (single crystal  $Al_2O_3$ ) fibers have been used in gamma irradiation studies. Sapphire-based FO cables have demonstrated negligible attenuation to 3.39 MGy [19]. Silica-based FO cables have demonstrated up to 115 dB/km of attenuation at 150 Mrad(SiO<sub>2</sub>) [20]. Thermal annealing has been shown to affect the attenuation of silica-based fiber [21] and sapphire-based fiber [22].

Connectors are a main point of failure in electronics systems. Consequently, careful consideration is required when selecting connectors for multi-conductor cables. Cable connectors are fabricated to match cable impedance by using the mating connector geometries and materials selected. Insulation integrity is just as critical for connectors as is with the cables. Furthermore, for nuclear reactor applications, connectors must be selected with considerations for robotic manipulation (if the connector must be replaced without

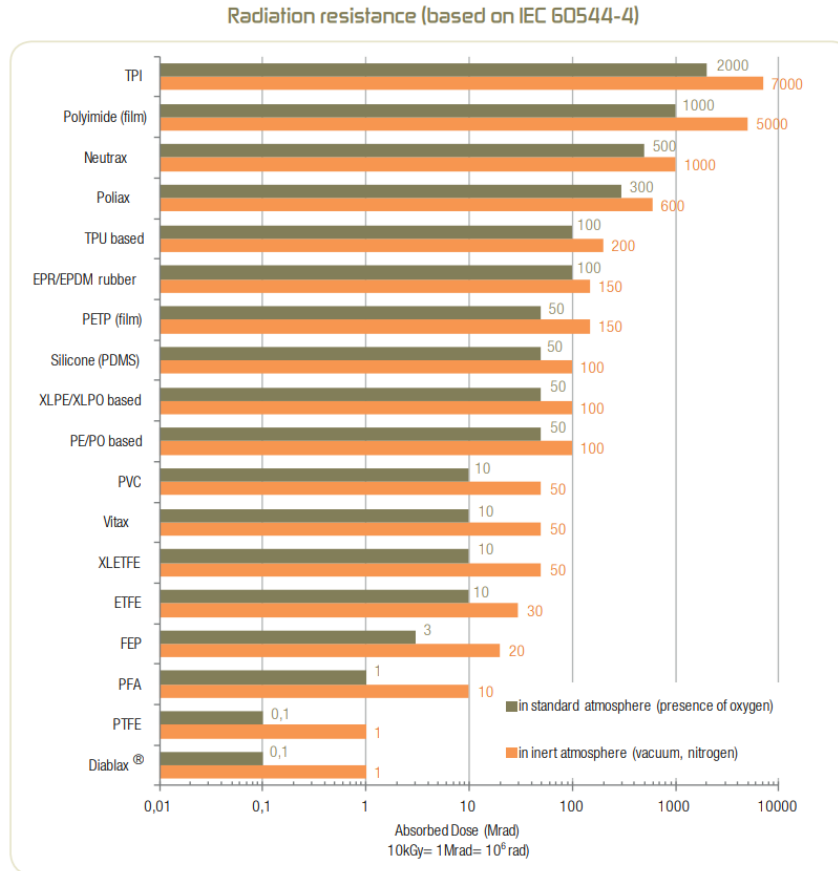


**Figure 4. Comparison of the radiation resistance of cable dielectric materials [13].**

direct human intervention due to the hazards of the target environment).

### 2.1.3 Inductors and Printed Circuit Boards

Gamma dose-rates have been shown to increase leakage currents of resistors by charge trapping effects. Conversely, charge trapping due to neutrons increase resistivity of conductors [9]. These damages are likely to be temporary due to material self annealing.

The magnet wire used in inductors and transformers is typically insulated with polyimide, which has shown survive to 100 MGy [13]. If insulated with another common material, please refer to the handbook by Hanks and Hamman [10]. Permanent magnets have low vulnerability to  $10^{17}$  n/cm<sup>2</sup> [23]. Similarly, magnetic materials such as silicon-steel and soft ferrites show negligible changes to the same magnitude of neutron fluence. However, some soft magnetic alloys, such as supermalloy, show major changes in permeability and coercive force at  $10^{16}$  n/cm<sup>2</sup> [23].

Printed circuit boards (PCBs) enable close integration of electrical components with increased signal integrity. Mechanical, electrical, and magnetic properties of PCBs have been studied recently [24]. Permittivity changes showed less than 3.5% variation over a thermal neutron fluence of  $1.1 \times 10^{16}$  n/cm<sup>2</sup> and gamma

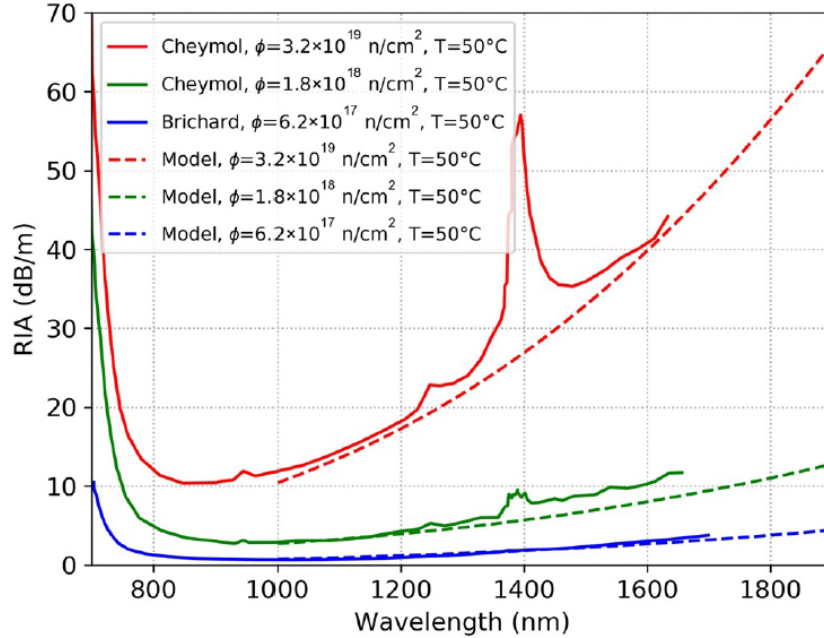


**Figure 5. Measured RIA of SiO<sub>2</sub> FO cables by Cheymol et al. [17] and Brichard et al. [18] with a radiation-induced compaction model [16].**

TID of 250 kGy. The dielectric constant of the PCBs insulating substrates such as FR4 or Rogers board governs trace impedance, which is critical for signal integrity. The substrate dielectric constants are resistant to neutron fluence and ionizing radiation, with increases of less than 0.75% at  $1.1 \times 10^{16}$  n/cm<sup>2</sup> (thermal), and 250 kGy with Rogers board showing the largest variations. These changes are attributed to the board's physical expansion due to radiation effects.

## 2.2 DISCRETE ACTIVE DEVICES

Modern electronics cannot rely on passive devices alone. Active devices serving as amplifiers, switches, and nonlinear devices are needed. An electronics engineer must understand the physics of active devices, along with their applications and their respective susceptibilities and limits due to irradiation, to design effective electronics and systems for the nuclear reactor environment. Table 3 provides an overview of the neutron degradation of selected discrete active devices through the associated the device fluence limits and the displacement damage effects on the present SOA devices. Similarly, Table 4 summarizes the gamma accumulated dose effects on devices and their respective TID limits. Please note that the information in these tables discusses the present maximum limits of these devices. Not all devices in a category will survive these limits or be useful for every application. Further information on the device physics, radiation failure mechanisms, and limits are discussed further this section.

**Table 3. Neutron displacement damage on active device technologies.**

Technology	Max fluence (n/cm <sup>2</sup> )	Displacement effects
Diodes	10 <sup>13</sup> – 10 <sup>15</sup>	Increased leakage currents; increased forward voltage threshold
LEDs	10 <sup>12</sup> – 10 <sup>14</sup>	Reduced light intensity
BJTs	10 <sup>13</sup>	Current gain degradation (PNP devices are more sensitive than NPN devices)
JFETs	10 <sup>14</sup>	Increased channel resistivity; decreased carrier mobilities
SiC JFET	10 <sup>16</sup>	Increased channel resistivity; decreased carrier mobilities
MOSFETs	10 <sup>15</sup>	Increased channel resistivity; decreased carrier mobilities
CMOS	10 <sup>15</sup>	Increased channel resistivity; decreased carrier mobilities

**Table 4. Gamma TID damage on active device technologies.**

Technology	TID (Gy)	TID Effects
Photodiodes	10 <sup>4</sup> – 10 <sup>6</sup>	Increased photocurrents
LEDs	10 <sup>5</sup> – 10 <sup>6</sup>	0.25 dB attenuation
BJTs	10 <sup>3</sup> – 10 <sup>5</sup>	Current gain degradation and increased leakage currents
JFETs	>10 <sup>6</sup>	Minimal observable effects
SiC JFET	>10 <sup>6</sup>	Minimal observable effects
Si MOSFETs	10 <sup>4</sup>	Increasing threshold voltage and leakage currents
CMOS	10 <sup>6</sup>	Variations in threshold voltage and leakage currents

### 2.2.1 Diodes, LEDs, and Photodiodes

A diode is a two-terminal (anode and cathode) nonlinear active device formed from a pn junction—a semiconductor material in which a region of the semiconductor crystal is doped to increase the number of holes (p-type), and an adjacent region of the crystal is doped to increase the number of electrons (n-type). The cross section of the p-n junction diode is shown in Figure 6. Since the hole concentration is large in the p<sup>+</sup> region and low in the n<sup>-</sup> region, holes diffuse from the p-side to the n-side of the device. Conversely, electrons that are highly concentrated in the n<sup>-</sup> region diffuse to the p<sup>+</sup> region. This majority-carrier diffusion is commonly known as *diffusion current*  $I_D$ . When the device terminals are left open, holes and electrons at the junction recombine to form a depletion region, establishing an electric field opposing the diffusion of holes to the n<sup>-</sup> region and electrons to the p<sup>+</sup> region. Thermally generated holes in the n material drift towards the junction where they reach the edge of the depletion region and are swept across the region to the p<sup>+</sup> side due to the established electric field. Similarly, minority electrons are generated thermally and move across to the n region. These minority-carrier currents form the drift current  $I_S$ .

Diodes operate within four different modes: open-circuit or equilibrium, forward-bias condition, reverse-bias condition, and breakdown. With no external voltage applied to the device, the magnitudes of the opposing diffusion current and drift current are equivalent, as the barrier voltage  $V_0$  is established with the n<sup>-</sup> region becoming more positive than the p<sup>+</sup> region, thereby limiting the diffusion current. The barrier

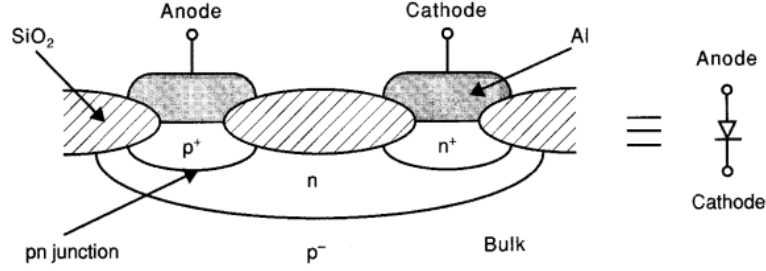


**Figure 6. Cross section of a p-n junction diode [25].**

voltage is given by

$$V_0 = V_T \ln \left( \frac{N_A N_D}{n_i^2} \right), \quad (1)$$

where  $V_T$  is the thermal voltage ( $V_T = k_B T / q$ ), and  $N_A$  and  $N_D$  are the doping concentrations of the  $p^+$  and  $n^-$  sides respectively. In these equations,  $k_B$  is the Boltzmann constant,  $T$  is the temperature in Kelvin, and  $q$  is the charge of an electron. This built-in junction voltage is usually in the range of 0.6 to 0.9 V. As a positive voltage is applied from anode to cathode (forward biasing the device), the depletion region width and barrier voltage decrease. As this barrier voltage decreases, the diffusion current begins to overcome the drift current and can conduct substantial currents. When a negative voltage is applied across the anode to the cathode (reverse biasing the diode), the depletion region and the barrier voltage increase. This decreases the magnitude of the diffusion current. The drift current overcomes the diffusion current. As the drift current is dependent on thermally generated minority carriers, the magnitude remains small. The current of an ideal diode operating in these three modes is given by

$$I = I_S (e^{V/V_T} - 1), \quad (2)$$

where  $I$  is the current flowing from the anode to the cathode. The fourth mode of a diode's operation, the reverse breakdown, occurs when a substantial negative voltage is applied across the diode, dramatically increasing the reverse current in either the avalanche or Zener method [26].

The most important parameters of diodes are the forward voltage drop, the reverse current, and the reverse breakdown voltage, as each of these parameters is important for specific applications. The forward voltage drop is critical in rectifier efficiency and protection circuits. Reverse current is used in photodetection applications. Reverse breakdown is often used to clamp voltages in power devices. In these devices, lattice degradation caused by displacement damage creates additional trapping centers that increase the material resistivity. This causes the forward voltage drop to increase with neutron fluence. In rectifying and power applications, this can reduce the power rating and efficiency of the device. Lattice damage also creates variations in the reverse breakdown voltage, resulting in voltage offset errors when using Zener diodes as voltage references. Electron-hole pairs formed near the junction of a semiconductor proportional to the incident ionizing radiation rate create photocurrents in the device that interfere in photosensitive applications.

The abundant charge carriers within a given region are called *majority carriers*, while the less abundant charges are referred to as *minority carriers*. As diodes (except Schottky-type) are minority-carrier devices, their lattice damage can be modeled by the *minority carrier lifetime*, which is defined as the average time for a hole injected into the  $n^-$  region to recombine with a majority electron. The relationship between neutron

displacement degradation and minority-carrier lifetime is expressed as follows:

$$\frac{1}{\tau_{\Phi}} = \frac{1}{\tau_i} + \frac{\Phi}{K_{\tau}}, \quad (3)$$

where  $\tau_{\Phi}$  is the minority-carrier lifetime after exposure,  $\tau_i$  is the initial minority-carrier lifetime,  $\Phi$  is the incident radiation fluence ( $\text{n/cm}^2$ ), and  $K_{\tau}$  is the damage constant ( $\text{n}\cdot\text{s}\cdot\text{cm}^{-2}$ ).

Rating diodes for radiation tolerance is challenging, because the diodes in each system have unique applications. It is important for the design engineer to understand the specific radiation effects on the diodes for their particular application. Si-based diodes have been shown to vary their forward voltage drop exponentially due to radiation, with the forward voltage drop increasing by an order of magnitude between neutron fluences of  $10^{13}$   $\text{n/cm}^2$  and  $10^{15}$   $\text{n/cm}^2$  [27].

Ionizing radiation produces free-charge carriers that establish photocurrents in diodes [27]. Photocurrents are current flowing in the reverse direction across a p-n junction. Photodiodes make use of photocurrents for sensing, receiving optical-based communications, and opto-coupling devices. Photodiodes are sensitive to variations in photocurrents. Photocurrents have been shown to vary by as much as three orders of magnitude in photodiodes with 10 kGy (Si) or as little as a factor of 5 with 440 kGy (Si) [28]. Knowing the photocurrent gamma relationship is critical for photodiode selection for applications in nuclear environments.

Displacement damage in light-emitting diodes (LEDs) manifests as decreased luminous intensity following the minority-carrier lifetime. These devices reach 50% intensity between fluences of  $10^{12} - 10^{14}$   $\text{n/cm}^2$  [29, 30]. However, LEDs used as general purpose diodes are insensitive to ionizing radiation and have shown as little as 0.28 dB attenuation at 290 kGy (Si) [28].

## 2.2.2 Bipolar Junction Transistors

Bipolar junction transistors (BJTs) are devices that employ a three-section alternating polarity structure of doped semiconductors to form a three-terminal (base, collector, emitter) active device. The device is commonly used as a voltage-controlled amplifier or switch by modulating the voltage across the base and emitter region. Figure 7 illustrates a detailed cross section of the device structure. This figure is using  $\text{n}^+$  doped material as the emitter, p doped as the base, and  $\text{n}^+$  doped as the collector. The base is a very thin layer between the heavily doped emitter and the more lightly doped collector. This configuration is known as an *NPN* bipolar transistor, and the opposite can also be employed, which would result in a *PNP* transistor.

The transistor functions by an injection of holes from the base into the emitter, which results in a larger emitter current of electrons diffusing into and across the base and into the collector. The ratio of electrons from the emitter and holes into the base is determined by doping levels during device design and is a critical performance parameter. Some of the holes in the base recombine with electrons moving through the base from the emitter to the collector, which reduces the total number of electrons and therefore reduces the current that exits the collector. The ratio of collector current to base current is the prime figure of merit of a bipolar transistor and is called  $h_{FE}$  or the *common-emitter current gain*.

BJTs can be operated in one of four modes, depending on the junction biasing conditions. In forward-active mode (active mode), the base-emitter junction is forward biased, and the base-collector junction is reverse biased. Most BJTs are optimized for operation in this mode. Reverse-active mode occurs when the base-emitter junction is reverse biased, and the base-collector junction is forward biased (opposite biasing that

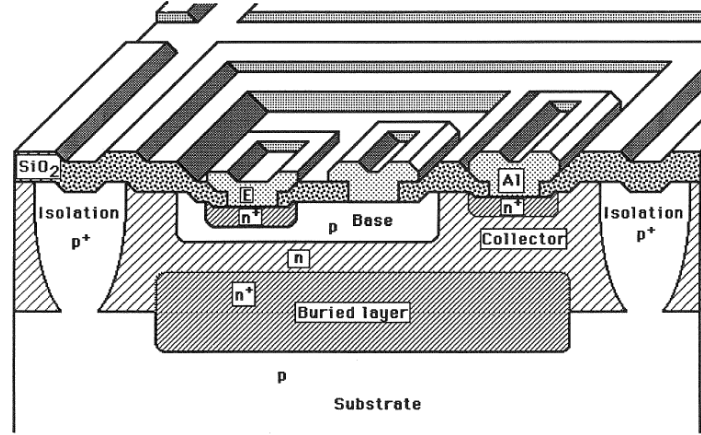


Figure 7. Cross section of an NPN BJT. [31]

switches the emitter and collection regions role). Saturation mode occurs when both junctions are forward biased. In this mode, the transistor may conduct high currents, making it suitable for use as a switch, thus rendering the BJT in the ON state. The opposite of the saturation mode is the cut-off mode, in which both junctions are reverse biased, and the transistor is in the OFF state.

The collector current  $I_C$  for a BJT in the forward-active region is expressed as

$$I_C = I_{CS} \left( 1 + \frac{V_{CE}}{V_A} \right) e^{V_{BE}/V_T}, \quad (4)$$

where  $V_{BE}$  represents the base-emitter voltage,  $V_{CE}$  is the collector-emitter voltage,  $I_{CS}$  is the transport saturation current in the forward direction,  $V_T$  is the thermal voltage  $V_T = k_B T/q$ , and  $V_A$  is the early voltage in the forward direction.

Since neutron irradiation creates mid-band traps due to dislocation defects, the hole and electron recombination rate in the base increase as a result of neutron irradiation which reduce the current gain,  $h_{FE}$ . This is seen as a current-dependent effect since the number of traps at a given time is fixed, but as the collector current decreases with bias, a greater fraction of the electrons crossing the base exhibit recombination, thus giving rise to decreasing  $h_{FE}$  as the collector current decreases. Modern transistors now tend to be more resistant to this effect since the base width and therefore the amount of time the electrons spend in the base region is reduced, thus allowing less time for recombination to occur. BJTs have been shown to survive neutron fluences of  $10^{13}$  n/cm<sup>2</sup> and gamma irradiation of 30 kGY [32–35].

### 2.2.3 Metal-Oxide-Semiconductor Field Effect Transistors

A metal-oxide-semiconductor field-effect transistor (MOSFET) is a four-terminal (gate, source, drain, body) active electronic device that uses a gate voltage to modulate conduction between the drain and the source. Applying a voltage to the oxide-insulated gate induces an electric field that affects the charge distribution in the channel, thus modifying its current conduction properties. MOSFETs can be constructed as either n-type or p-type devices, each of which can be configured to be an enhancement mode (normally off) or depletion mode (normally on) device. In an enhancement mode device, a conductive channel does not exist between

the gate and drain, and a positive voltage is required to create a conductive path (in an n-type MOSFET). In a depletion mode device, a conductive channel is present in the device, with no applied gate to source voltage ( $V_{GS}$ ), and an applied  $V_{GS}$  is used to reduce or eliminate the current passing from the drain to the source. For an enhancement mode n-type device, the threshold voltage ( $V_{th}$ ) represents the required  $V_{GS}$  to induce current flow between the source and drain so that when  $V_{GS} \geq V_{th}$ , inversion of the channel occurs. In this scenario, the majority carriers in the channel are depleted by the applied  $V_{GS}$ , and the minority carriers are attracted towards the gate, forming a conduction path between the source and the drain. Note that the body terminal of the device plays a small role in device operation, as it has a secondary effect on the device threshold voltage ( $V_{th}$ ). A cross section of an NMOS device is shown in Fig. 8.

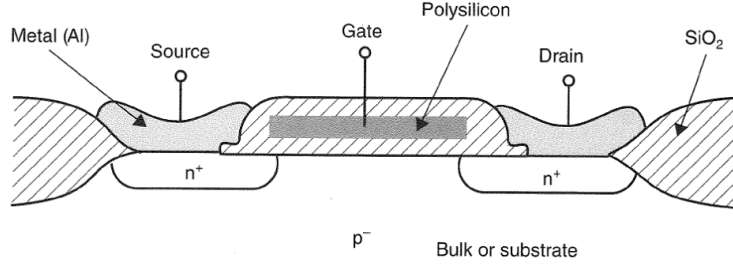


**Figure 8. Cross section of NMOS transistor [25].**

Three separate modes of operation exist for the MOSFET based on the applied gate voltage ( $V_{GS}$ ) and applied drain to source voltage ( $V_{DS}$ ): subthreshold mode, triode mode, and saturation mode. Subthreshold (often called *cutoff* or *weak-inversion*) mode applies when the gate-to-source voltage is less than the voltage threshold of the device ( $V_{GS} < V_{th}$ ), and the drain current  $I_D$  follows

$$I_D \approx I_{D0} e^{\frac{V_{GS} - V_{th}}{nV_T}}, \quad (5)$$

where  $I_{D0}$  is the current at  $V_{GS} = V_{th}$ ,  $V_T$  is the thermal voltage ( $V_T = kT/q$ ) and the slope factor  $n$  is given by

$$n = 1 + \frac{C_{dep}}{C_{ox}}, \quad (6)$$

where  $C_{dep}$  is depletion layer capacitance, and  $C_{ox}$  is the gate oxide capacitance. In triode mode (also called *linear region* or *ohmic mode*), when  $V_{GS} > V_{th}$  and  $V_{DS} < V_{GS} - V_{th}$ , the drain current is approximated as

$$I_D = \mu_n C_{ox} \frac{W}{L} \left[ (V_{GS} - V_{th}) V_{DS} - \frac{V_{DS}^2}{2} \right] (1 + \lambda V_{DS}), \quad (7)$$

where  $\mu_n$  is the charge-carrier mobility,  $W$  is the gate width,  $L$  is the gate length, and  $\lambda$  is the channel-length modulation parameter.

Saturation mode (also referred to as *active mode*) applies for  $V_{GS} > V_{th}$  and  $V_{DS} > V_{GS} - V_{th}$ . The drain current in saturation follows:

$$I_D = \frac{\mu_n C_{ox} W}{2 L} [V_{GS} - V_{th}]^2 [1 + \lambda (V_{DS} - V_{DS_{sat}})]. \quad (8)$$

In each mode, the drain current produced has a unique relationship with  $V_{GS}$ . In the subthreshold mode, the drain current varies exponentially with  $V_{GS}$ . The linear region drain current is approximately proportional to  $V_{GS} - V_{th}$ . The saturation mode drain conduction current is proportional to the square of  $V_{GS} - V_{th}$ .

The three modes of operation for all MOSFET types have common mechanisms of operation: applied voltages create electric fields that redistribute semiconductor charges and govern the conduction characteristics of the channel. Unwanted phenomena such as radiation exposure can negatively impact device performance and stability over time due to charge deposition. Similarly, threshold voltage shifts may occur due to trapped charge in the gate oxide layer or the surrounding field oxide. In extreme circumstances, large amounts of induced charge can produce currents that limit device performance or induce damage. Lattice damage may also occur, resulting in reduced device performance and increased device noise due to the addition of charge trapping locations in the conductive channel region.

Because they are majority carrier devices, neutron damage is less significant in MOS structures than in BJTs. MOS damage is induced primarily from ionizing radiation, with the threshold voltage being the most sensitive parameter [36]. The increasing threshold voltage is attributed to field creation on the Si-SiO<sub>2</sub> interface from charge traps. These changes are typically temporary and will recover with annealing. MOS devices have been shown to have radiation resilience to 10 kGy (Si) TID, 10 MGy (Si)/s dose rate, and fluence of 10<sup>15</sup> n/cm<sup>2</sup> [9]. Modern rad-hard research on discrete FETs primarily focuses small feature CMOS processes and on WBG semiconductor material processes, which are discussed further in Section 2.2.6.

## 2.2.4 Complementary Metal-Oxide-Semiconductor Technology

Complementary MOS (CMOS) combines MOS transistors of both polarities into a single device. The fabrication and cross section is illustrated in Figure 9. The NMOS transistor is implemented on a p-type substrate, while the PMOS transistor is placed into an n-well. An oxide region is used to isolate the devices from each other. The complementary nature of the CMOS transistor with the NMOS device acting as a pull-down and the PMOS device acting as a pull-up allows the transistor to be implemented as push-pull amplifiers without the necessity of using load resistors. This implementation yields relatively high-gain amplifiers and optimizes the power requirements. At the present time, CMOS dominates the market over either single NMOS or PMOS devices for analog, digital, and mixed signal integrated circuits (ICs).

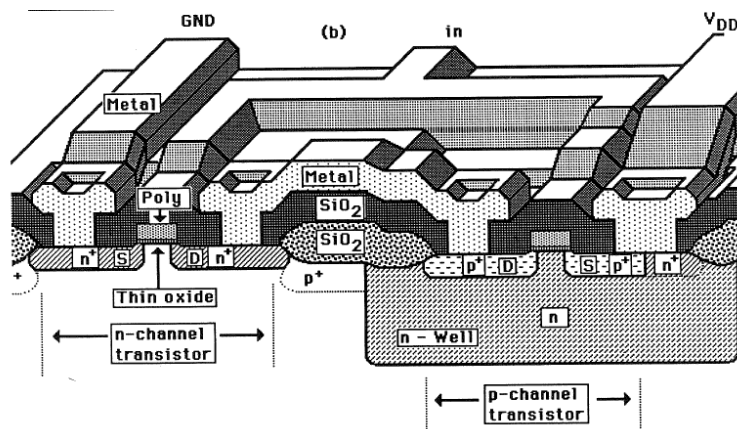


Figure 9. CMOS process cross section [31].

CMOS devices function on the same governing principles as their single PMOS and NMOS transistor implementations, and they suffer from the same radiation effects and limitations. However, because of their increased amplifier efficiencies, NMOS and PMOS devices are usually implemented for power switching,

requiring a larger physical footprint, while CMOS circuits target high density, very low-power applications such as digital processing architectures, resulting in reduced device footprints. As predicted by Moore's law, the physical sizes of these devices and their respective oxide-layers have decreased over time. As their physical dimensions have decreased, their sensitivity to gamma-induced charge trapping has also decreased, but their sensitivity to SEEs due to dose-rate have increased. Using modern deep-submicron processes with appropriate device layout/design, gamma TIDs of 1 MGy can be expected. The goal of the present research is for a device to survive greater than 10 MGy [37, 38].

## 2.2.5 Junction Field Effect Transistors

Junction field-effect transistors (JFETs), like bipolar transistors, are bulk-semiconductor devices, which means that their performance characteristics are determined primarily by the bulk properties of the semiconductors rather than thin conductive interfaces, as in MOSFET devices. Therefore, the effects of radiation are generally mitigated, making JFET devices excellent candidates for many rad-hard applications.

JFETs function in a manner similar to MOSFETs in that an electric field modulates a conductive channel through which current flows. A cross section drawing of a p-channel JFET (pFET) is shown in Figure 10. The drain and source contacts are connected to the p-doped channel which is surrounded by an n-doped gate. The p-doped channel is fabricated with a known cross sectional area defined by the n-type diffusing regions on each side of the p-type channel. The device gate is formed by electrically connecting the two n-type regions. The typical circuit configuration of a pJFET is for the drain to be biased more negatively than the source and the channel modulation to be defined by the voltage of the gate to be equal to or greater than the source. As the gate voltage increases, a depletion region between the gate and channel develops which reduces the cross sectional area of the channel. If the gate voltage is increased sufficiently, then the depletion region extends across the entire channel and stops the current flow in a phenomenon referred to as *pinch-off*. The gate-to-source voltage  $V_{GS}$  where current flow is halted is known as *the pinch-off voltage* ( $V_p$ ).

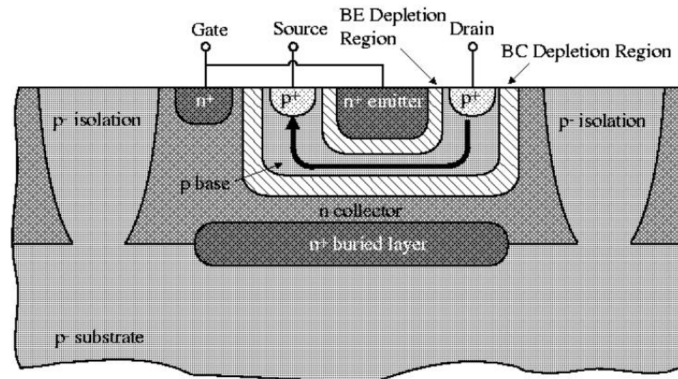


**Figure 10. Cross section of pJFET transistor [39].**

The JFET is normally considered a depletion-mode device because the conductive channel exists for a gate-source voltage of 0 V, and it is reduced as the gate voltage is increased for a pFET. A JFET that is constructed of the opposite semiconductor polarities that are used in a pFET is called an *nJFET*. In contrast to the pFET, the nFET depletion region increases with decreasing  $V_{GS}$ . Therefore, the nFET drain current decreases as

$V_{GS}$  decreases. For an nFET, the region where  $V_{GS} \leq V_P$  is known as the cutoff, and the drain current  $I_D = 0$ . The triode region occurs when  $V_P \leq V_{GS} \leq 0$  and  $V_{DS} \leq V_{GS} - V_P$ . In the triode mode of operation, the drain current is defined by

$$I_{DS} = I_{DSS} \left[ 2 \left( 1 - \frac{V_{GS}}{V_P} \right) \left( \frac{V_{DS}}{V_P} \right) - \left( \frac{V_{DS}}{V_P} \right)^2 \right], \quad (9)$$

where  $V_{GS}$  is the gate-source voltage,  $I_{DS}$  is the drain current,  $I_{DSS}$  is the drain current at  $V_{GS} = 0V$ ,  $V_P$  is the pinch-off voltage, and  $V_{DS}$  is the drain to source voltage [26]. Saturation of the nFET occurs when  $V_P \leq V_{GS} \leq 0$  and  $V_{DS} \geq V_{GS} - V_P$ ; the drain current follows:

$$I_{DS} = I_{DSS} \left( 1 - \frac{V_{GS}}{V_P} \right)^2 (1 + \lambda V_{DS}), \quad (10)$$

where  $\lambda$  is the inverse of the early voltage  $\lambda = 1/V_A$ , and  $V_A$  and  $\lambda$  are positive for nFET devices.

The voltage-current characteristics of the pFET behave in a manner similar to the nFET device, with opposing polarities. For the pFET,  $V_P$  is positive,  $\lambda$  and  $V_A$  are negative,  $0 \leq V_{GS} \leq V_P$ ,  $V_{DS}$  is negative, and the drain current  $I_D$  flows from the source to the drain. The pFET is in saturation when  $V_{DS} \leq V_{GS} - V_P$ , and it is operating in the triode region when  $V_{DS} \geq V_{GS} - V_P$ .

Generally, JFETs are extremely rad-hard to both displacement and ionization damage due to both the bulk structure and the normally high level of doping [40]. Threshold voltage variations observed in MOSFETs are negligible in JFETs, which are not fabricated with the gate oxide insulating layer. Little change has been shown for ionization doses of up to 10 MGy and neutron fluences of  $>10^{14}$  n/cm<sup>2</sup> [33, 41].

### 2.2.6 Wide Bandgap Devices

Electronics devices fabricated with WBG semiconducting substrates have been a target of research. Silicon-carbide (SiC) and gallium nitride (GaN) devices have been emerging in the market for power electronics and RF applications. Devices fabricated with these materials can operate at greater temperatures than Si-based devices, making them strong candidates for oil and gas applications.

Using WBG-based semiconducting devices is enticing for nuclear power applications. Because their bandgap energy is greater than that of Si-based devices, the energy required to create electron-hole pairs and thus charge traps is greater. Also, these materials can have greater doping, as the device breakdown voltages are greater than for Si-based devices, which increases the neutron hardness of WBG-based devices.

The work by McGarrity et al. indicates that SiC-JFETs improved the neutron fluence to  $10^{16}$  n/cm<sup>2</sup>, which is two orders of magnitude greater than traditional Si-JFET devices [42]. GaN is another WBG material of interest. Enhancement-mode GaN FETs have shown resistance to neutron fluences  $>10^{15}$  n/cm<sup>2</sup>, and GaN-based LEDs have shown increases in shown neutron fluence degradation to  $>10^{16}$  n/cm<sup>2</sup> [43, 44].

### 2.2.7 Vacuum Devices

Vacuum tube devices were introduced in the late 19<sup>th</sup> and early 20<sup>th</sup> centuries. Unlike transistors, vacuum tubes operate by the production of free electronics by thermionic emissions. Current flow is controlled by

modulating the electric fields in the electron path. Commercial vacuum tubes have been developed for an assortment of applications over the years such as radio and RF applications, audio, cameras, and televisions. It is a common misconception that all vacuum tubes require several hundred volts or more for operation; there were many tubes developed for 12 V operation due to the advent of radio receiver development for automobiles in the middle of the 20<sup>th</sup> century. With the advent of the transistor and especially CMOS integrated circuits, vacuum tubes began losing market space. Tubes are still being manufactured, primarily for audio applications. These devices have been refined, but their basic functionality remains unchanged [45].

Recent interest and revival of tube technologies have been sparked. As electron mobility of these devices is limited by the field effects on electrons, vacuum tubes become applicable in very high frequency applications (terrahertz region). Tube size has been a negative factor in their applications, as many billions of transistors can be monolithically applied in a single IC chip. Small micro- and nano-scale tubes have been tried with various levels of success and have been tested to gamma doses of 2.5 MGy without observable changes [46, 47]. However, these were not detailed tests, as they omitted detailed operational data. More recently, thermionic devices without a vacuum channel present have been under development [48] in which the electron path length is small enough that there is negligible probability of electron-air molecule collisions.

## **2.3 INTEGRATED CIRCUITS**

ICs increase the design efficiency of electronic systems by reducing engineering costs and time to market while typically reducing the overall system size and often power consumption. Space and satellite applications dominate the commercial and research IC component markets, with few components exceeding ratings and testing to 1–10 kGy. Testing for neutron sensitivities of these devices is rare, as neutron radiation is not generally applicable to the space or low earth orbit (LEO) environment. Generally, radiation vulnerabilities follow levels and effects similar to those discussed in Section 2.2, with CMOS and bipolar CMOS (BiCMOS) increasing the radiation resistance due to smaller device feature size and proper use of rad-hard by process (RHBP) and rad-hard by design (RHBD) engineering practices.

### **2.3.1 Voltage Regulators and Power Devices**

Sensors and associated electronics have various power, voltage, and current requirements. Common devices often feature various voltages to accommodate many applications. For instance, microcontrollers may require somewhere between 2–5 V of direct current (VDC), while amplifiers may need 12 VDC or greater for their operations. Energy and power supplies may also vary, depending on applications. Batteries may produce an output voltage between 2.8–3.5 VDC, while associated electronics and sensors may require less. Integrated power converters have been developed to manage these voltage and power conversions. Power conversion circuits can be classified into four categories: DC-DC conversion, DC-AC inverters, AC-AC converters, and AC-DC rectifiers.

Historically DC-DC converters used linear regulators to step down a voltage. Applications requiring low-noise power rails still use these devices, although their efficiency is limited. Modern switched-mode DC-DC converters use inductors or transformers with power transistors to take advantage of the inductor physics by rapidly switching currents through the inductor. This fast switching can be used to step up (boost) or step down (buck) voltages. At the output, an appropriately sized output filtering capacitor smooths the voltage

switching into the desired DC voltage with some minimal AC ripple, typically on the order of a few percent of the DC voltage.

DC-AC inverters switch the DC voltage in a manner similar to DC-DC converters. However, they manipulate the duty-cycle of the their devices to produce a sinusoidal output waveform. Many of these devices use transformers for isolation and to act as the low-pass filter to smooth out the high-frequency switching content.

AC-AC conversion has traditionally been performed by using the turns ratios of transformers to step up or step down the voltage. Modern high efficiency AC-AC converters first rectify the signal, and using high efficiency switch-mode DC-DC converters, they convert the signal to the desired voltage level before inverting it back to AC. When this method is properly implemented, it increases efficiency by reducing transformer core losses. AC-DC converters either feature a transformer to step up or step down the AC voltage to the desired level and then rectify the signal, or they first rectify the AC input and then convert it using high-efficiency DC-DC converters.

Low-dropout voltage regulators and other voltage converters based on BiCMOS devices have been shown to resist 10–300 kGy (SiO<sub>2</sub>) TID and neutron fluence of 10<sup>13</sup> n/cm<sup>2</sup> [49–53]. Buck converters using a 250 nm CMOS process reliably perform to 1 MGy with little observable effects [54].

### **2.3.2 Operational Amplifiers**

Operational amplifiers (opamps) are one of the most versatile building blocks in analog electronics. The first monolithic commercial opamp was produced in 1963 (uA702 opamp, Fairchild Semiconductor), and since then, many thousands of designs have been commercially available and widely used. Before IC capabilities were developed, opamps were constructed using vacuum tubes, which required the use of high voltages, and they were very large, power inefficient, and expensive. The advancement of IC technology starting in the 1950s enabled increasingly high levels of device integration, in turn enabling mass production and utilization of these circuits. Presently, there are more than 1,000 monolithic opamps available commercially. Commercial opamps are commonly packaged as single, dual, or quad devices, and they are rated for one of three temperature ranges: commercial (0 to 70°C), industrial (-40 to 70°C), and military (-55 to 125°C). In addition to commercially produced, individually packaged opamps, designs are commonly found as building blocks in much larger integrated circuit products.

The real utility of opamps becomes apparent when they are configured with negative feedback using external devices. Using negative feedback, the overall function of the opamp circuit and associated characteristics, such as input and output impedance, voltage gain, and frequency response, can be precisely determined by external feedback components such as capacitors and resistors.

Ideal opamps are often used for straightforward circuit analysis, and they commonly include the following ideal characteristics: infinite input impedance, infinite differential voltage gain, infinite slew rate and bandwidth, zero output impedance, zero input offset voltage, and zero input-referred noise. In addition, ideal opamps operate over any voltage range and have an infinite power supply rejection ratio (PSSR), as well as a common mode rejection ratio (CMRR). Although actual devices do not exhibit these characteristics, modern circuit and process design enable realization of extremely capable circuits that can be used very effectively.

Opamps can be used to construct many common circuits, including voltage followers, inverting and non-inverting amplifiers, inverting and non-inverting summing circuits, differentiators, integrators, differential amplifiers, transimpedance or transconductance (current-to-voltage or voltage-to-current) amplifiers, instrumentation amplifiers, negative resistance circuits, variable gain amplifiers, and envelope and peak detector circuits. Opamps are also commonly used to form active filters, including low-pass, high-pass, and bandpass types (e.g., Sallen-Key topologies) with configurable transition band characteristics, including Butterworth, Chebyshev, elliptical, and many other types. These precise filter functions are realized using an opamp with external passive devices.

Commercially available opamps are often categorized to help designers select from the huge number of different opamp designs available. Common categories of opamps include general purpose, precision, rail-to-rail, current feedback (vs. voltage feedback), high output current drive, high bandwidth, extended voltage, low input noise, JFET input, low power, low input bias current, and low drift. As opamp designs have advanced, the associated simulation tools and device models have progressed, as well. Most contemporary opamp designs that are still in production provide extensive simulation models for their opamps, suitable for use with common simulation program with integrated circuit emphasis (SPICE) analog circuit simulation tools, including LTSPICE, PSPICE, HSPICE and others.

Opamps are the one of most multifaceted analog components, so there are numerous detrimental radiation mechanisms to be considered when designing with them, and the radiation limits are difficult to ascertain without considering the application of the device. The behavior and reliability of 500 nm CMOS opamps under ionizing radiation are the subject of a study by Cardoso et al. [55]. It is important to note that these behaviors are subject to the opamp design, including RHBD techniques implemented in the cell libraries. Hogue et al. present a 10 kGy TID CMOS cell library for designing analog components such as opamps and comparators [56].

### 2.3.3 Analog and Digital Converters

Analog-to-digital converters (ADCs) and digital-to-analog converters (DACs) bridge the gap between the analog and digital signal worlds. These can be featured as standalone ICs or as part of a larger VLSI circuit such as a microcontroller. Both device types are governed by sampling theory and require precision timing and clock circuits.

Many functional types of ADCs exist. The common topologies are flash, successive approximation, single or multi-slope integration, and delta-sigma. In *flash* ADCs, the input voltage is applied to a set of  $2^n$  comparators, where  $n$  is the number of bits in the conversion against a set of fixed reference voltages. *Successive approximation* ADCs use internal DACs to apply a set of trial codes of size  $n$  in quick succession to be compared with the analog voltage signal. These are conventionally implemented as an  $R$ - $2R$  successive approximation resistor network or with ratioed capacitors. *Single-* and *multi-slope* ADCs convert an analog signal by measuring the time required for an internally generated analog ramp or set of ramps to equal the value of the analog input signal. *Delta-sigma* converters are the most popular because they can reduce noise, but at the cost of complexity. In this type of converter, a modulator converts the analog input voltage into a series of sequential bits that are streamed to a digital low-pass filter, producing the  $n$ -bit digital output. Significant increases in effective resolution can be achieved using this architecture due to its innovative use of noise shaping and oversampling operations.

Like ADCs, there are many types of DACs, each with unique advantages. The types considered here are

resistor strings,  $R$ - $2R$  resistor ladders, binary-scaled current sources, as well as pulse-averaging and sigma-delta converters. *Resistor-string* converters consist of a set of  $2^n$ -matched resistors connected between a stable voltage reference and ground, with a set of voltage controlled switches (typically MOSFETs) connecting a single resistor node (referred to as a *tap*) to an output buffer. As seen, the number of equally matched resistors grows exponentially with the number of bits, limiting the practical size of these converters.  $R$ - $2R$  ladders collapse the quantity of resistors needed to an array of size  $2n$ . These converters implement a ladder network of matched resistors with values of  $R$  and  $2R$ , and they switch the appropriate binary-weighted resistor output into a summing amplifier. *Current-steering* converters, as the name suggests, output a current instead of a voltage to increase the speed of conversion. Currents are driven by an array of transistor current sources with scaled emitter resistors, commonly in an  $R - 2R$  ladder. *Pulse-averaging* DACs operate by generating a pulse-width modulated signal followed by a low-pass filter, with frequency cutoff equal to the pulse width modulation (PWM) interval (carrier) frequency. Modulating the width of a fixed clock interval pulse to correspond to the output voltage value and filtering effectively averages the voltage in the clock period to the correct voltage level. For instance if the pulse width is set to 5 V for 25% of the clock cycle and 0 V for the remaining 75%, then the output voltage would average to 1.25 V after filtering. *Sigma-delta* converters work on a similar principle, except the pulse width is fixed, and a number of sequenced on and off pulses are output to a low-pass filter with a frequency cutoff well below the clock cycle.

Research into rad-hard ADCs that survive the greater ionizing doses found in space applications is focused on CMOS processes. Broell et al. designed an 8-bit CMOS ADC which was shown to withstand between 5 and 10 kGy (Si) [57]. A successive approximation ADC is being developed by Ro et al. using a 130 nm CMOS process and radiation simulation software [58]. Ro's ADC has been simulated to 1 MGy (Si) with promising results. Kuppambatti et al. have demonstrated a 12-bit 40 MS/s ADC prototype irradiated to 107 kGy (Si) and proton fluence of  $10^{14}$  p/cm<sup>2</sup> based on a 130 nm CMOS process [59]. Research into rad-hard DACs is more limited to space applications. Sordo-Ibanez et al. tested a 350 nm CMOS DAC that showed resistance to  $>3$  kGy (Si) [60].

### 2.3.4 Digital and Mixed Signal Integrated Circuits

Digital logic gates represent the foundational building blocks of digital circuitry. These gates are Boolean algebra devices and can be cascaded to form adders, multipliers, multiplexers, encoders, flip-flops, etc. Very large-scale integration (VLSI) circuits such as microcontrollers and field programmable gate arrays (FPGAs) are built on these basic building blocks.

Discrete digital logic devices are built as transistor-transistor logic (TTL) or CMOS logic, CMOS being the most common and energy efficient. Typically, these devices operate using 3.3 or 5 V logic levels. BJT-based logic devices are more susceptible to neutrons and dose-rate SEEs, whereas CMOS devices are more sensitive to ionizing radiation and dose-rate SEEs. In digital circuits, SEEs manifest as latch-up events and increases in signal propagation times. Latch-ups are events of an erroneous bit occurring in the logic circuits. These are overwritten during the next write cycle. Common techniques such as triple-modular redundancy are used in rad-hard digital circuitry to mitigate these errors using a majority voting scheme.

Microprocessors and microcontroller units (MCUs) are programmable digital or mixed-signal devices consisting of hundreds of thousands to billions of transistors. These VLSI ICs are used in a broad array of applications such as controls, sensing, communications, computing, and digital signal processing. Design costs are reduced through rapid prototyping, as the reprogrammable nature of these general purpose devices

allows for various algorithms to be programmed without a complete hardware rework.

MCUs are general purpose computational devices which include an excess of internal peripheral ICs enabling use in many applications. FPGAs provide a massive array of replicated configurable logic blocks having Boolean logic gates, memory, flip flops, and in some cases, digital signal processing (DSP)-specific hardware. A highly programmable interconnect array structure with signal bus and clocking channels allows highly custom configuration of these very capable devices. FPGAs do not feature the same general purpose overhead circuits that are common to MCUs, thus enabling higher performance operation for many digital signal processing or control functions. Many variations of FPGAs are commercially available, ranging from extremely fast, high-density products (e.g., Xilinx Vertex, and Kintex families) to very low power, much less capable programmable devices (Xilinx Coolrunner II CPLD). Use of the highest performance/density FPGAs comes at the cost of increased design effort, although modern software tools are shortening the design process times.

Application-specific integrated circuits (ASICs) are custom-integrated circuits that can be process and design optimized for maximum performance and energy utilization. These devices are not typically used for general purposes, as they are designed for very specific tasks. Engineering design time and fabrication costs of ASIC devices are much greater than for the previously mentioned devices. As such, they are generally recommended for large market applications in which these nonrecurring engineering costs can be distributed over many sold units (often millions), or in power critical applications such as distributed sensor networks.

Research of rad-hard MCUs are focused on RHBD techniques and creation of standard cell libraries to achieve TIDs of  $>1\text{kGy}$  [61–63]. It is unclear whether these devices have been fabricated and tested to evaluate their performance under irradiation. However, research on FPGAs has shown that devices based on the CMOS process achieve greater than  $20\text{ kGy}$  ( $\text{SiO}_2$ ) [64]. Research into these VLSI devices is focused on sub-micron CMOS processes for increasing TID and methods for mitigating SEEs for space applications.

### **2.3.5 Data-Links and Communication Interfaces**

Device internal and external data links are crucial for large-scale systems integration. Internal data links focus on data flow between registers, memory, internal arithmetic, and logic structures. These include the protocol stack, direct access memory, and cache. Internal data links are commonly instigated in a parallel bus of conductors. However, serial links exist and are frequently implemented as external data links. Serializers-deserializers (SERDES) exist to convert data between the parallel and serial architectures.

External serial data links sequentially transmit a buffer or stack of bits across a few conductors or optical fiber with high bit rates over a point-to-point link. Serial peripheral interface (SPI) is a commonly used four-wire synchronous serial communication interface with high baud rates. This architecture features full-duplex data transfer controlled by a serial select line with a shift register timing controlled by a supplied clock. Inter-integrated circuit ( $I^2C$ ) is a half-duplex two-wire serial data link architecture that uses addressing instead of multiple serial select lines, which decreases the conductor overhead by sacrificing speed. Joint test action group (JTAG) standard, USB, and asynchronous RS-232 are other common serial data links used in IC communications.

External parallel buses use multiple data lines to transfer data from one device to another. These architectures can transfer data at high rates, but they require larger physical space requirements to implement. Common

examples of these interfaces include peripheral component interconnect (PCI), general purpose integrated bus (GPIB), and small computer system interface (SCSI).

The gigabit transceiver (GBT) family of custom integrated circuits has been specifically designed for high-energy physics applications by a research group in Cern Switzerland. These designs provide three primary functions common to many detector systems: slow data acquisition and control (GBT-SCA, 1 MGy TID), serializer/de-serializer function (GBTx, 1 MGy TID), and bidirectional or dual transmitter optical communications, including optical driver and receiver (VTTx, 4.8 Gb/s, 500 kGy TID,  $5 \times 10^{14}$  particles/cm<sup>2</sup>) [65]. All chips/modules are also qualified for -55 to 125°C operation. These designs demonstrate the potential of using CMOS processes with RHBD and triple modular redundancy (TMR) techniques to meet the very challenging environments associated with nuclear reactors.

### 2.3.6 Commercial IC Offerings

Commercially available ICs are dominated by the market for space applications. As discussed in Section 1.1, protons, GCRs, and ionizing radiation are the dominant types of radiation in the satellite and space exploration environments. A significant but limited array of rad-hard (>10 kGy) and rad-tolerant (1–3 kGy) devices is available from commercial vendors, including Analog Devices, Honeywell Aerospace, Xilinx, TI, Maxwell Technologies, Renesas, BAE Systems, and STMicroelectronics. These devices specifically target the LEO satellite market for rad-hard electronics, and they are used in limited space flight applications, as well.

Renesas has an extensive line of rad-tolerant devices intended for satellite and space applications. A selection of their components, including communication interfaces, microprocessors, FETs, current sources, and amplifiers, is found in Table 6. Space-rated components are also developed and sold by BAE Systems including memory, power management, FPGAs, and microprocessors, and a selection of these components is found in Table 7. TI advertises an extensive line of space-rated rad-hard devices. Table 9 presents an overview of a few of their selection of parts, including ADCs, DACs, power converters and management, sensing, logic, opamps, MCUs, and communications. Xilinx specializes in FPGAs. They offer a couple of rad-tolerant FPGAs, as well as a rad-hard FPGA, as shown in Table 8. STMicroelectronics features a selection of space-rated components, as shown in Table 5. Their selection includes discrete transistors, data converters, diodes, logic gates, communication interfaces, and PWM controllers. These tables do not provide an exhaustive list of the components available from their respective vendors; nor do these tables represent the complete market of commercially available ICs and components.

**Table 5. Commercial space-rated device offerings from STMicroelectronics [66]**

<b>Part class (#)</b>	<b>Description</b>	<b>Rad specifications</b>	<b>Temp (°C)</b>
BJTs (14)	-	1 kGy TID	-55 to 125
Data converters (3)	ADCs, 8-bit, up to 50 MSps, up to 8-ch	3 kGy TID (Si), SEL 125 (MeV-cm <sup>2</sup> /mg)	-55 to 125
Data converters (1)	DAC, 24-bit, up to 3 MSps, up to 8-ch	1 kGy TID (Si), SEL 125 (MeV-cm <sup>2</sup> /mg)	-55 to 125
Diodes & rectifiers (18)	Schottky and bipolar	30 kGy TID	-65 to 150
Logic (209)	Families: 54AC/ACT, 54HC/HCT, 54VCX, CMOS 4000B	0.5 - 3 kGy TID	-55 to 125
LVDS (8)	400 Mbit/s LVDS drivers, receivers, serdes	3 kGy TID SEL 135 (MeV-cm <sup>2</sup> /mg)	-55 to 125
Opamps & comparators (9)	Low noise, low power, high speed	3 kGy TID	-55 to 125
Voltage regulators (7)	Adjustable and fixed	3 kGy TID	-55 to 150
Gate Drivers (2)	Dual low-side MOSFET drivers	1 kGy TID SEL 60 (MeV-cm <sup>2</sup> /mg)	-55 to 125
PWM controllers (2)	Current mode PWM controllers	0.5 - 1 kGy TID	-55 to 150
MOSFETs (6)	N-channel MOSFET P-channel MOSFET	500 Gy TID 1000 Gy TID	-55 to 150
Voltage references (2)	1.2V and 2.5–5.0V references	3 kGy TID	-55 to 125

**Table 6. Commercial space-rated device offerings from Renesas–Intersil [67]**

Part class (#)	Description	Rad specifications	Temp (°C)
Interface (1)	CMOS programmable peripheral interface	1 kGy SEL 50 MeV-cm <sup>2</sup> /mg	-55 to 125
Microprocessor (1)	16-bit CMOS microprocessor	1 kGy	-35 to 125
GaN FETs (4)	Gallium nitride field effect transistors	1 kGy (2) HDR SEL 86 MeV-cm <sup>2</sup> /mg	-55 to 125
GaN FET drivers (2)	Gallium nitride FET drivers	1 kGy (1) HDR SEL 86 MeV-cm <sup>2</sup> /mg	-55 to 125
Current sources (4)	100 $\mu$ A and 1 mA precision current sources	1 kGy (2) HDR	-55 to 125
Amplifiers	Instrumentation amplifiers (2)	750 Gy LDR	-55 to 125
Op-amps	Single and quad operational amplifiers (2)	300 Gy LDR	-55 to 125
Voltage regulator (3)	6–18 A synchronous buck converters	1 kGy HDR	-55 to 125
Voltage regulator	Low dropout regulator	1 kGy HDR (1)	-55 to 125

**Table 7. Commercial space-rated device offerings from BAE Systems [68]**

Part class (#)	Description	Rad specifications	Temp (°C)
Memory (1)	Magnum 4-MB static RAM	5 kGy TID, $1 \times 10^{13}$ particles/cm <sup>2</sup>	-55 to 125
Memory (1)	Non-volatile RAM, 256k $\times$ 20	5 kGy TID (Si), $1 \times 10^{13}$ particles/cm <sup>2</sup>	-55 to 125
Memory (1)	Programmable ROM 32k $\times$ 8	2 kGy TID (Si), $1 \times 10^{12}$ particles/cm <sup>2</sup>	-55 to 125
Memory (1)	Synchronous FIFO, 1k $\times$ 36	5 kGy TID (Si), $1 \times 10^{13}$ particles/cm <sup>2</sup>	-55 to 125
Power management (1)	RAD POLX DC-DC converter, 88% efficiency	500 Gy TID (Si)	-55 to 125
FPGA (2)	Field programmable gate array	1–1.5 kGy TID (Si)	-55 to 125
Microprocessor (1)	RAD750 power PC microprocessor	2 kGy TID (Si)	-55 to 125

**Table 8. Commercial space-rated device offerings from Xilinx [69]**

Part class (#)	Description	Rad specifications	Temp (°C)
FPGA	RT Kintex Ultrascale FPGA	1 kGy TID (Si), SEL >80 (MeV-cm <sup>2</sup> /mg)	-55 to 125
FPGA	Virtex-4QV FPGA	3 kGy TID (Si), SEL >125 (MeV-cm <sup>2</sup> /mg)	-55 to 125
FPGA	Virtex-5QV FPGA	10 kGy TID (Si), SEL >125 (MeV-cm <sup>2</sup> /mg)	-55 to 125

**Table 9. Commercial space-rated device offerings from Texas Instruments [70]**

Part class (#)	Description	Rad specifications	Temp (°C)
ADCs (4)	RF sampling ADCs, single/dual, 8-bit 3.0 GSPS to 12-bit 6.4 GSPS	3 kGy TID, Max SEL 120 (MeV-cm <sup>2</sup> /mg)	-55 to 125
ADCs (1)	24-bit, 8-ch sigma delta, simultaneous sampling	750 Gy TID, Max SEL 68 (MeV-cm <sup>2</sup> /mg)	-55 to 125
DACs (4)	12-bit to 24-bit, up to 2.4 GSPS	1 kGy TID, Max SEL 109 (MeV-cm <sup>2</sup> /mg)	-55 to 125
Power Management (16)	Voltage regulators (LDO, Adj., Fixed), Voltage References (diode, shunt), Step-down converters, Buck converters, PWM controllers	1 kGy TID	-55 to 125
Sensing (1)	Current shunt monitor, temperature sensor	1 kGy TID, Max SEL 76 (MeV-cm <sup>2</sup> /mg)	-55 to 125
Logic (73)	Full family of logic gates, drivers, flip-flops, multiplexers	Space grade, No further irradiation data	-55 to 125
Opamps (12) & Comparators(5)	Family of opamps, comparators	400-1000 Gy	-55 to 125
Opamps (4)	Single and dual	3 kGy TID, Bipolar	-55 to 125
RF PLL (1)	40 MHz to 15 GHz wideband synthesizer	1 kGy TID, Max SEL 120 (MeV-cm <sup>2</sup> /mg)	-55 to 125
MCUs (1)	MSP430 mixed signal microcontroller	500 Gy TID, Max SEL 72 (MeV-cm <sup>2</sup> /mg)	-55 to 125
DSPs (2)	Floating point digital signal processor	1 kGy TID	-55 to 125
Memory	16-MB static RAM	3 kGy TID, Max SEL 100 (MeV-cm <sup>2</sup> /mg)	-55 to 125

## 2.4 SYSTEMS

### 2.4.1 Cameras

Video cameras are based on one of two primary methods of transduction. The first method is the cathode ray tube (CRT) scanning approach. An image is electrically reconstructed using a beam of electrons to sense varying degrees of intensity. The various types (image orthicons, vidicons, and others) are typically differentiated by the technique they use for reading out the imaging plate [15]. These types of cameras are good for extremely high total dose applications because of the inherently high threshold of radiation tolerance of vacuum electronics [71].

More recently, solid-state light sensors such as charge-coupled devices (CCDs) or complementary metal oxide semiconductor (CMOS) active pixel sensors (APSs) use the photo-sensitivity semiconductors to generate images. Solid-state cameras have better resolution and power requirements, but they are not usually rad-hard. Even when they have been hardened, they tend to have dose capabilities that are two to three orders of magnitude lower than CRT-based cameras [15]. Pushing the limits on these cameras, researcher organizations want cameras that are rad-hard to at least 10 MGy. Recent offerings by Mirion include cameras for reactor environments that are rated up to 2 MGy [72].

### 2.4.2 Power Conversion and Harvesting Systems

A rad-hard energy harvesting and through-wall communications system targeted for dry-cask monitoring was developed through a collaboration between ORNL, Virginia Tech, and the University of North Texas [73]. This Si-based electronics system has been tested to 20 kGy (Si), with the energy harvester and piezoelectric transducer elements tested to 1 MGy (Si). Currently, high-temperature testing and further irradiation testing of the Si-based electronics system is underway. This system is pushing the envelope for extremely high TID electronics, sensor and communications, and energy harvesting systems

### 2.4.3 Communications and Controls

ORNL is leading the development of rad-hard electronics for the International Thermonuclear Experimental Reactor (ITER) service vacuum system. This system monitors and controls a large number of vacuum lines, and it incorporates circuits for analog-to-digital conversion, digital input/output, and high speed bidirectional Gb/s fiber optics-based serial communications. ORNL's present system prototype electronics are designed for use in the wall mounted cubicle (WMC), and they utilize 100 krad TID radiation-tolerant voltage regulators (Texas Instruments) and GBT family slow serial controller (GBT-SCA), serializer deserializer (GBTX), and fiber optic transceiver units (VTRx) based on custom ICs from research groups in Cern, Switzerland. The GBT-SCA and GBTX are rated  $\geq 1$  MGy TID, and the VTRx ICs are rated at 500 Gy TID and  $5 \times 10^{14}$  n/cm<sup>2</sup> [65].

Flexible, reconfigurable, software-defined radios (SDRs) have redefined communications research. Communication structures and protocol stacks can be rapidly redefined. Cognitive radio that employs machine learning techniques has garnered recent interest for dynamic spectrum allocation and cyber security [74]. Recently, BAE Systems developed a rad-hard (10 kGy TID) software-defined radio for space applications based on their RAD5545<sup>TM</sup> single board computer [75].

#### **2.4.4 Robots and Remote Operations**

Robotics and remote operations are commonly used in nuclear environments to prevent unnecessary exposure to humans. Typical operations for these applications are repetitive tasks that can be fully automated. Robotics are used to shorten the time required for reactor maintenance and to minimize worker time in hazardous areas. In most cases, robots have been designed for intermittent use or only when absolutely needed. These robots are not required to be as radiation-tolerant as a robot created to manipulate radioactive equipment on a daily basis [76].

The Semi-Intelligent Mobile Observing Navigator (SIMON) was a monitoring vehicle developed in 1990 that was used at the Savannah River Site to measure radiation and temperature and to retransmit televised views of the area [77]. The SIMON design is radiation tolerant up to a total dose of 200 Gy. This is one example of an intermittent use robot. Other robots were used for waste storage monitoring, inspection and cleaning of steam generators, reactor vessel inspections, pipe inspections, underwater inspections, handling and processing of waste materials, decontamination and decommissioning (surface cleaning), and tank cleaning. For decommissioning, the robots were radiation resistant up to 10 kGy from  $^{137}\text{Cs}$  by use of tungsten shielding [78]. Several of these robots use the rad-hard camera technology discussed in previous sections. Robots and robotic vehicles are employed when accidents happen in nuclear environments and during post-accident operations such the Chernobyl accident on April 26, 1986 [77]. These robots and robotics vehicles still could not be used longer term in radiation environments, but have pushed the development of rad-hard electronics.

A prototype electronics platform for rad-hard robot applications was previously developed at ORNL through the DOE Nuclear Energy Enabling Technologies (NEET) program. This system incorporated a configurable analog front end, two analog-to-digital converters, and a serial link integrated into a custom ASIC. Two prototype units were radiation tested at Arizona State University and functioned correctly through 3 kGy TID testing.

Several radiation hardening strategies have been used, including modification of existing designs (extensive testing, identification, and replacement of radiation sensitive parts) and innovative designs (complete re-design of the system incorporating radiation tolerant devices). Radiation hardening design techniques used for robots and robotic vehicles include the appropriate component selection of commercial-off-the-shelf (COTS) parts, radiation-tolerant designs, natural annealing, and biasing or unbiasing of devices.

### **3. GAPS AND FUTURE DIRECTIONS IN NUCLEAR RADIATION HARDENED ELECTRONICS**

As the SOA of rad-hard electronics research and device ratings are extending into the ranges of MGy TID and  $10^{16}$  n/cm<sup>2</sup> neutron fluences, potential applications in nuclear environments are abundant. However, progress in several technical focus areas is needed to accelerate realization of the next generation radiation hardened electronics suitable for present and future nuclear reactor applications. In this section, specific technology gaps limiting further progression of rad-hard electronics for nuclear reactors are identified, and associated potential technical directions for mitigating these deficiencies are discussed.

Commercially available rad-hard component offerings are only qualified and tested for LEO and space applications, where GCRs are most prevalent, and neutrons are sparse. Total ionizing dose resistance for these

components is only characterized to 3–10 kGy, which is sufficient for space applications. Irradiating components to greater radiation magnitudes or including neutrons are not economical approaches for space-rated devices. The neutron and ionizing radiation environment requirements for electronics in nuclear reactors dwarf those of space applications.

Modern commercial electronics fail to support placement of sensor electronics in close proximity to cores. Near- or in-core placement of sensors is becoming more desirable for existing and advanced reactor designs and irradiation experimentation. Placing rad-hard electronics closer to their respective sensors increases the signal-to-noise-plus-interference ratios (SNIRs) associated with long cabling by digitizing or amplifying the signal before additive noise is injected. Higher SNIRs thereby increase the attainable precision and accuracy of sensors. However, radiation and temperature effects cause erroneous interference to the electronics devices through threshold voltage and current gain variations, SEEs (bit-errors), current leakage, and delays attributed to accumulated dose and dose rate. To optimize system SNIR, careful mapping of the radiation environment and electronics system lifetimes must be addressed.

Reactor radiation and temperature environmental mapping with associated classification of electronic resistances is scarce. Efficient solutions for the next generation of rad-hard electronics will require an extensive assessment of reactor and cask environments. While radiation and temperature maps have been created for specific reactor facilities, no standard requirements have been established for gamma and neutron exposure or for temperature. To make progress in this field, it is essential that radiation standards be established for target neutron and gamma radiation accumulated doses, dose rates, and temperature limits for electronic device qualifications of various nuclear applications.

There is no database of reactor-qualified components and devices unavailable to electronic designers. Presently, commercially available components and systems are qualified for space flight/satellite applications rather than for the unique radiation and temperature environments of nuclear reactors. A publicly available detailed list or database detailing the component offerings available and their radiation and temperature limits from the commercial sector should be created. Development of this list could begin with the re-qualification of commercially available space-grade components for target nuclear environments and should extend into commercial off-off-the-shelf (COTS) and research community devices. Maintenance of this list will require consistent diligence.

Mechanisms for transitioning rad-hard electronics from the research sector to the industrial sector are needed. In addition to commercially offered rad-hard devices and circuits, several highly rad-hard designs have been published by the research community that are directly applicable to the reactor environment. Means for transitioning these designs for common use in reactors should be developed. This effort will require government support, as the commercial integrated circuit sector has not embraced rad-hard electronics for reactors due to the extremely limited market.

In general, the rad-hard electronics devices and systems presently qualified for space flight/satellite applications lag far behind standard commercial products in terms of functional complexity and degree of integration. A system-on-chip (SoC)-based approach which integrates common platform capabilities (ADC, DAC, signal processing, digital IO, and communications) onto a single chip would provide a widely applicable device for reactor sensing and control platforms. Limited functional programmability—by fuse programming or by serial communications-based programming—would advance the utilization of this design.

While Si-based systems are very mature and have adequate temperature performance to meet the requirements of space applications, reactor temperature ranges can far exceed those of standard Si fabrication pro-

cesses. However, as discussed in Section 1.2, temperatures in reactor environments are increasing for each new generation to increase the thermal efficiency of the power plants. Rad-hard devices and systems qualified to exceed 125–150°C are needed for these higher temperature environments, but commercial offerings for high-temperature and rad-hard electronics are scarce. WBG-based electronics systems have higher temperature ratings than comparable Si-based systems, but with lower technology maturity than that required for a near- or in-core reactor environment. The larger bandgap energies associated with WBG devices allow for increased doping due to their greater voltage breakdown limits. Increased doping creates greater resistance to neutron fluence by maintaining functionality when lattice atoms are displaced for a period long enough to allow for in-situ thermal recombination and annealing, which is accelerated by the higher temperatures of reactor environments. WBG devices should be researched further for potential use in nuclear reactor or spent fuel applications.

Wireless systems for communication in near-core environments do not exist. Cabling provides for a long lifetime, but efforts to maintain and access the cables create significant expenses compared to the efforts required for simple wireless device replacement. Reducing cabling quantities and length decreases associated costs while increasing SNIR for cases in which electronics can be placed in close proximity to sensors. Data can be transmitted through high-speed wireless systems, but high-speed wireless communication systems are not commercially available for the reactor market, and they also suffer from severe attenuation when signalling through containment structures. More advanced, highly integrated, rad-hard data communications blocks must be developed for RF and through-containment data telemetry and control in the reactor environment. This functionality may also be integrated into an SoC design for further integration of all system functions.

#### **4. CONCLUDING REMARKS**

This report presents and discusses the current state-of-the-art rad-hard systems and devices for nuclear applications and identifies areas for future development. Space and nuclear radiation environments are summarized to elaborate on the device degradation effects caused by radiation, to evaluate the current state-of-the-art research, and to identify possible methods, candidate electronics architectures, or existing space-rated technologies for nuclear applications. A better standardization of the application environment requirements to address radiation and temperature effects is needed to successfully and efficiently develop, test, and qualify the technology essential for nuclear application spaces. Once these qualifications are established, commercially available devices and systems currently in use can then be tested for their intended environments, and a database of nuclear-rated electronic equipment can be developed. Devices and materials under research can be added to this database to establish partnerships between commercial partners, national laboratories, and universities to accelerate rad-hard electronics development. Meanwhile, further development of discrete active devices and integrated circuits is possible. This work could leverage existing commercially available products, implementing radiation hardening through design and process techniques with existing inexpensive materials and through further investment in WBG materials development.

## 5. REFERENCES

- [1] R. Velazco, D. McMorrow, and J. Estela, *Radiation Effects on Integrated Circuits and Systems for Space Applications*. Springer, 2019.
- [2] M. Durante and F. A. Cucinotta, “Physical basis of radiation protection in space travel,” *Reviews of Modern Physics*, vol. 83, no. 4, p. 1245, 2011.
- [3] E. Stassinopoulos and J. P. Raymond, “The space radiation environment for electronics,” *Proceedings of the IEEE*, vol. 76, no. 11, pp. 1423–1442, 1988.
- [4] K. A. LaBel, A. H. Johnston, J. L. Barth, R. A. Reed, and C. E. Barnes, “Emerging Radiation Hardness Assurance (RHA) Issues: A NASA Approach for Space Flight Programs,” *IEEE Transactions on Nuclear Science*, vol. 45, no. 6, pp. 2727–2736, 1998.
- [5] R. Johnson, F. Thome, and C. Craft, “A Survey of Aging of Electronics with Application to Nuclear Power Plant Instrumentation,” *IEEE Transactions on Nuclear Science*, vol. 30, no. 6, pp. 4358–4362, 1983.
- [6] *Light Water Reactor Sustainability (LWRS) Program*, (accessed September 23, 2020). [Online]. Available: <https://www.energy.gov/ne/nuclear-reactor-technologies/light-water-reactor-sustainability-lwrs-program>
- [7] S. J. Zinkle and G. Was, “Materials Challenges in Nuclear Energy,” *Acta Materialia*, vol. 61, no. 3, pp. 735–758, 2013.
- [8] R. Viswanathan, “Materials Technology for Coal-Fired Power Plants,” *Advanced Materials and Processes*, vol. 162, no. 8, pp. 73–80, 2004.
- [9] G. C. Messenger and M. S. Ash, *The Effects of Radiation on Electronic Systems*. Van Nostrand Reinhold Company Inc., 1986.
- [10] C. Hanks and D. Hamman, “Radiation Effects Design Handbook. Section 3: Insulating Materials and Capacitors,” *NASA, Washington DC*, 1971.
- [11] J. Laghari and A. Hammoud, “Effect of Nuclear Radiation on the Electrical Properties of Chemical Double Layer Capacitors,” *IEEE Transactions on Nuclear Science*, vol. 37, no. 2, pp. 1072–1075, 1990.
- [12] A. Di Buono, N. Cockbain, P. R. Green, and B. Lennox, “The Effects of Total Ionizing Dose Irradiation on Supercapacitors Deployed in Nuclear Decommissioning Environments,” *Journal of Power Sources*, vol. 479, p. 228675, 2020.
- [13] *Axorad Radiation Resistant Cables for Scientific & Nuclear Applications*, 2018 (accessed September 17, 2020). [Online]. Available: [https://www.axon-cable.com/publications/AXORAD\\_CABLESANG.pdf](https://www.axon-cable.com/publications/AXORAD_CABLESANG.pdf)
- [14] L. Vermeeren and R. Van Nieuwenhove, “Theoretical Study of Radiation Induced Electromotive Force Effects on Mineral Insulated Cables,” *Review of Scientific Instruments*, vol. 74, no. 11, pp. 4667–4674, 2003.

- [15] D. E. Holcomb, C. L. Britton Jr, V. K. Varma, and L. G. Worrall, "Remote Operations and Maintenance Framework for Molten Salt Reactors," Oak Ridge National Lab.(ORNL), Oak Ridge, TN (United States), Tech. Rep., 2018.
- [16] C. M. Petrie, A. Birri, and T. E. Blue, "High-Dose Temperature-Dependent Neutron Irradiation Effects on the Optical Transmission and Dimensional Stability of Amorphous Fused Silica," *Journal of Non-Crystalline Solids*, vol. 525, p. 119668, 2019.
- [17] G. Cheymol, H. Long, J. F. Villard, and B. Brichard, "High Level Gamma and Neutron Irradiation of Silica Optical Fibers in CEA OSIRIS Nuclear Reactor," *IEEE Transactions on Nuclear Science*, vol. 55, no. 4, pp. 2252–2258, 2008.
- [18] B. Brichard, P. Borgermans, A. F. Fernandez, K. Lammens, and A. Decreton, "Radiation Effect in Silica Optical Fiber Exposed to Intense Mixed Neutron-Gamma Radiation Field," *IEEE Transactions on Nuclear Science*, vol. 48, no. 6, pp. 2069–2073, 2001.
- [19] D. Sporea and A. Sporea, "Radiation Effects in Sapphire Optical Fibers," *Physica Status Solidi C*, vol. 4, no. 3, pp. 1356–1359, 2007.
- [20] M. Kyoto, Y. Chigusa, M. Ohe, H. Go, M. Watanabe, T. Matsubara, T. Yamamoto, and S. Okamoto, "Gamma-Ray Radiation Hardened Properties of Pure Silica Core Single-Mode Fiber and Its Data Link System in Radioactive Environments," *Journal of Lightwave Technology*, vol. 10, no. 3, pp. 289–294, 1992.
- [21] C. M. Petrie, D. P. Hawn, W. Windl, and T. E. Blue, "Reactor radiation-induced attenuation in fused silica optical fibers heated up to 1000 c," *Journal of Non-Crystalline Solids*, vol. 409, pp. 88–94, 2015.
- [22] C. M. Petrie, W. Windl, and T. E. Blue, "In-Situ Reactor Radiation-Induced Attenuation in Sapphire Optical Fibers," *Journal of the American Ceramic Society*, vol. 97, no. 12, pp. 3883–3889, 2014.
- [23] D. Gordon and R. Sery, "Effects of Charged Particles and Neutrons on Magnetic Materials," *IEEE Transactions on Communication and Electronics*, vol. 83, no. 73, pp. 357–361, 1964.
- [24] K. Scheuer, J. Holmes, E. Galyaev, D. Blyth, and R. Alarcon, "Radiation Effects on FR4 Printed Circuit Boards," *IEEE Transactions on Nuclear Science*, 2020.
- [25] D. A. Johns and K. Martin, *Analog Integrated Circuit Design*. John Wiley & Sons, 2008.
- [26] A. Sedra, K. C. Smith, T. C. Carusone, and V. Gaudet, *Microelectronic Circuits 8th Edition*. Oxford University Press, New York, 2020.
- [27] C. Hanks and D. Hamman, "Radiation Effects Design Handbook. Section 1: Semiconductor Diodes." Battelle Memorial Inst., Columbus, Ohio. Radiation Effects Information Center, Tech. Rep., 1971.
- [28] H. Lischka, H. Henschel, W. Lennartz, and K. Schmidt, "Radiation Sensitivity of Light Emitting Diodes (LED), Laser Diodes (LD) and Photodiodes (PD)," *IEEE transactions on nuclear science*, vol. 39, no. 3, pp. 423–427, 1992.
- [29] A. Gradoboev, K. Orlova, I. Asanov, and A. Simonova, "The Fast Neutron Irradiation Influence on the AlGaAs IR-LEDs Reliability," *Microelectronics Reliability*, vol. 65, pp. 55–59, 2016.
- [30] C. Li and S. Subramanian, "Neutron Irradiation Effects in GaN-Based Blue LEDs," *IEEE Transactions on Nuclear Science*, vol. 50, no. 6, pp. 1998–2002, 2003.

- [31] W. Maly, *Atlas of IC technologies: An Introduction to VLSI Processes*. Benjamin-Cummings Pub Co, 1987.
- [32] G. E. Schwarze and A. Frasca, "Neutron and Gamma Irradiation Effects on Power Semiconductor Switches," 1990.
- [33] J. Assaf, R. Shweikani, and N. Ghazi, "Radiation Effect on Silicon Transistors in Mixed Neutrons-Gamma Environment," *Radiation Physics and Chemistry*, vol. 103, pp. 142–145, 2014.
- [34] J. Assaf, "Investigation of Irradiation Effect on npn BJT Electrical Properties," *Radiation Physics and Chemistry*, vol. 127, pp. 1–6, 2016.
- [35] H. F. Abdul Amir and F. P. Chee, "Evaluation on Diffusion of Bipolar Junction Transistor (BJT) Charge-Carrier and its Dependency on Total Dose Irradiation," in *Advanced Materials Research*, vol. 701. Trans Tech Publ, 2013, pp. 71–76.
- [36] J. Drennan and D. Hamman, "Radiation Effects Design Handbook. Section 4 - Transistors," 1971.
- [37] V. Goiffon, S. Rolando, F. Corbière, S. Rizzolo, A. Chabane, S. Girard, J. Baer, M. Estribeau, P. Magnan, P. Paillet *et al.*, "Radiation Hardening of Digital Color CMOS Camera-on-a-Chip Building Blocks for Multi-MGy Total Ionizing Dose Environments," *IEEE Transactions on Nuclear Science*, vol. 64, no. 1, pp. 45–53, 2016.
- [38] M. Menouni, M. Barbero, F. Bompard, S. Bonacini, D. Fougeron, R. Gaglione, A. Rozanov, P. Valerio, and A. Wang, "1-Grad Total Dose Evaluation of 65 nm CMOS Technology for the HL-LHC Upgrades," *Journal of Instrumentation*, vol. 10, no. 05, p. C05009, 2015.
- [39] *Circuit Symbols for JFETs*, (accessed September 26, 2020). [Online]. Available: <https://www.slideserve.com/zaria/circuit-symbols-for-jfets>
- [40] M. Citterio, S. Rescia, and V. Radeka, "A Study of Low Noise JFETs Exposed to Large doses of Gamma-Rays and Neutrons," in *IEEE Conference on Nuclear Science Symposium and Medical Imaging*. IEEE, 1992, pp. 794–796.
- [41] M. Citterio, J. Kierstead, S. Rescia, and V. Radeka, "Radiation Effects on Si-JFET Devices for Front-End Electronics," *IEEE transactions on nuclear science*, vol. 43, no. 3, pp. 1576–1584, 1996.
- [42] J. McGarrity, F. McLean, W. DeLancey, J. Palmour, C. Carter, J. Edmond, and R. Oakley, "Silicon Carbide JFET Radiation Response," *IEEE transactions on nuclear science*, vol. 39, no. 6, pp. 1974–1981, 1992.
- [43] A. Lidow, A. Nakata, M. Rearwin, J. Strydom, and A. Zafrani, "Single-Event and Radiation Effect on Enhancement Mode Gallium Nitride FETs," in *2014 IEEE Radiation Effects Data Workshop (REDW)*. IEEE, 2014, pp. 1–7.
- [44] A. Ionascut-Nedelcescu, C. Carlone, A. Houdayer, H. Von Bardeleben, J.-L. Cantin, and S. Raymond, "Radiation Hardness of Gallium Nitride," *IEEE Transactions on Nuclear Science*, vol. 49, no. 6, pp. 2733–2738, 2002.
- [45] P. Redhead, "The Birth of Electronics: Thermionic Emission and Vacuum," *Journal of Vacuum Science & Technology A: Vacuum, Surfaces, and Films*, vol. 16, no. 3, pp. 1394–1401, 1998.

- [46] D. Lynn and J. McCormick, “Progress in Radiation Immune Thermionic Integrated Circuits,” Los Alamos National Lab., NM (USA), Tech. Rep., 1985.
- [47] J. B. Mc Cormick, D. K. Wilde, S. W. Depp, D. J. Hamilton, and W. J. Kerwin, “Development of Integrated Thermionic Circuits for High-Temperature Applications,” *IEEE Transactions on Industrial Electronics*, no. 2, pp. 140–144, 1982.
- [48] S. Srisophonpan, Y. S. Jung, and H. K. Kim, “Metal-Oxide–Semiconductor Field-Effect Transistor with a Vacuum Channel,” *Nature nanotechnology*, vol. 7, no. 8, p. 504, 2012.
- [49] V. Vukić and P. V. Osmokrović, “Impact of Forward Emitter Current Gain and Geometry of PNP Power Transistors on Radiation Tolerance of Voltage Regulators,” *Nuclear Technology and Radiation Protection*, vol. 25, no. 3, pp. 179–185, 2010.
- [50] V. Đ. Vukić, “Minimum Dropout Voltage on a Serial PNP Transistor of a Moderately Loaded Voltage Regulator in a Gamma Radiation Field,” *Nuclear Technology and Radiation Protection*, vol. 27, no. 4, pp. 333–340, 2012.
- [51] J. Beaucour, T. Carriere, A. Gach, and D. Laxague, “Total Dose Effects on Negative Voltage Regulator,” *IEEE transactions on nuclear science*, vol. 41, no. 6, pp. 2420–2426, 1994.
- [52] G. Bonna, A. Bigga, B. Roberts, A. Imbruglia, F. Faccio, R. Duperray, P. Jarron, and M. Glaser, “A radiation-Hardened Low-Dropout Voltage Regulator for LHC and Space Applications,” CERN, Tech. Rep., 1999.
- [53] T. R. Oldham, C. M. Whitney, B. J. Griffiths, and N. van Vonno, “Summary and Analysis of Neutron Displacement Damage Results,” in *2018 IEEE Radiation Effects Data Workshop (REDW)*. IEEE, 2018, pp. 1–4.
- [54] S. Dhawan, O. Baker, H. Chen, R. Khanna, J. Kierstead, F. Lanni, D. Lynn, C. Musso, S. Rescia, H. Smith *et al.*, “Commercial Buck Converters and Custom Coil Development for the Atlas Inner Detector Upgrade,” *IEEE Transactions on Nuclear Science*, vol. 57, no. 2, pp. 456–462, 2010.
- [55] G. S. Cardoso, T. R. Balen, M. S. Lubaszewski, and O. L. Gonçalez, “Reliability Analysis of 0.5  $\mu\text{m}$  CMOS Operational Amplifiers under TID Effects,” *Journal of Integrated Circuits and Systems*, vol. 9, no. 1, pp. 70–79, 2014.
- [56] D. R. Hogue, G. A. Perry, S. R. Rumel, R. Bonebright, J. C. Braatz, M. Baze, and J. Holic, “A Rad-Hard Analog CMOS Cell Library,” in *2000 IEEE Radiation Effects Data Workshop. Workshop Record. Held in conjunction with IEEE Nuclear and Space Radiation Effects Conference (Cat. No. 00TH8527)*. IEEE, 2000, pp. 21–25.
- [57] F. G. Broell and W. J. Barnard, “A Radiation-Hardened CMOS 8-Bit Analog-to-Digital Converter,” *IEEE Transactions on Nuclear Science*, vol. 30, no. 6, pp. 4246–4250, 1983.
- [58] D. Ro, C. Min, M. Kang, I. J. Chang, and H.-M. Lee, “A Radiation-Hardened SAR ADC with Delay-Based Dual Feedback Flip-Flops for Sensor Readout Systems,” *Sensors*, vol. 20, no. 1, p. 171, 2020.
- [59] J. Kuppambatti, J. Ban, T. Andeen, P. Kinget, and G. Brooijmans, “A Radiation-Hard Dual Channel 4-Bit Pipeline for a 12-Bit 40 MS/s ADC Prototype with Extended Dynamic Range for the ATLAS Liquid Argon Calorimeter Readout Electronics Upgrade at the CERN LHC,” *Journal of Instrumentation*, vol. 8, no. 09, p. P09008, 2013.

- [60] S. Sordo-Ibáñez, B. Piñero-García, M. Muñoz-Díaz, A. Ragel-Morales, J. Ceballos-Cáceres, L. Carranza-González, S. Espejo-Meana, A. Arias-Drake, J. Ramos-Martos, J. M. Mora-Gutiérrez *et al.*, “CMOS Rad-Hard Front-End Electronics for Precise Sensors Measurements,” *IEEE Transactions on Nuclear Science*, vol. 63, no. 4, pp. 2379–2389, 2016.
- [61] M. Fossiona, A. Van Esbeena, T. Van Humbeecka, Y. Geertsb, E. Geukensb, S. Redantc, R. Jansend, and C. Monteleoned, “A Mixed-Signal Radhard Microcontroller: the Digital Programmable Controller (DPC) AMICSA 2014.”
- [62] B. De Muer, J. Dielens, E. Geukens, J. Van den Berk, D. Liebens, Y. Geerts, G. Thys, and S. Redant, “Radiation Hardened High-Voltage and Mixed-Signal IP with DARE Technology.”
- [63] S. Millnera, A. Zollera, and V. Luecka, “Using a Standard Commercial Process for Full Custom Rad Hard Mixed-Signal Design.”
- [64] L. Rockett, D. Patel, S. Danziger, B. Cronquist, and J. Wang, “Radiation Hardened FPGA Technology for Space Applications,” in *2007 IEEE Aerospace Conference*. IEEE, 2007, pp. 1–7.
- [65] P. Moreira, K. Wyllie, B. Yu, A. Marchioro, C. Paillard, K. Kloukinas, T. Fedorov, N. Pinilla, R. Bal-labriga, S. Bonacini *et al.*, “The GBT Project,” 2009.
- [66] *Space Products*, 2020 (accessed September 28, 2020). [Online]. Available: <https://www.st.com/en/space-products.html>
- [67] *Intersil Space Products*, Brochure, 2019 (accessed September 28, 2020). [Online]. Available: <https://www.renesas.com/us/en/doc/brochure/r30ca0174eu0300-space-products.pdf>
- [68] *Space Product Literature*, 2020 (accessed September 28, 2020). [Online]. Available: [https://www.baesystems.com/cs/ContentServer?packedargs=WEBROOTNAME%3Den\\_us&c=BAEStandardArticle\\_C&childpagename=US%2FBAELayout&rendermode=preview&pagename=USWrapper&cid=1434554746610](https://www.baesystems.com/cs/ContentServer?packedargs=WEBROOTNAME%3Den_us&c=BAEStandardArticle_C&childpagename=US%2FBAELayout&rendermode=preview&pagename=USWrapper&cid=1434554746610)
- [69] *Space*, 2020 (accessed September 28, 2020). [Online]. Available: <https://www.xilinx.com/applications/aerospace-and-defense/space.html#overview>
- [70] *TI Space Products*, Brochure, 2019 (accessed September 28, 2020). [Online]. Available: <https://www.ti.com/lit/sg/slyt532g/slyt532g.pdf?ts=1601265818682&>
- [71] *Eyes Inside: Radiation-Tolerant CCTV*, (accessed September 23, 2020). [Online]. Available: <http://www.neimagazine.com/features/featureeyes-inside-radiation-tolerant-cctv/>
- [72] *Radiation Tolerant Cameras*, 2020 (accessed September 23, 2020). [Online]. Available: [https://mirion.s3.amazonaws.com/cms4\\_mirion/files/pdf/brochures/web\\_ops-952\\_v.1a\\_nuclear\\_camera\\_matrix\\_-1-.pdf?1598974077](https://mirion.s3.amazonaws.com/cms4_mirion/files/pdf/brochures/web_ops-952_v.1a_nuclear_camera_matrix_-1-.pdf?1598974077)
- [73] Y. Wu, L. Zuo, S. Kaluvan, H. Zhang, M. N. Ericson, K. Reed, and R. A. Kisner, “Self-Powered Wireless Through-Wall Data Communication for Nuclear Environments,” Oak Ridge National Lab.(ORNL), Oak Ridge, TN (United States), Tech. Rep., 2019.
- [74] A. Anderson, S. R. Young, F. K. Reed, and J. M. Vann, “Deep Modulation (Deepmod): A Self-Taught PHY Layer for Resilient Digital Communications,” *arXiv preprint arXiv:1908.11218*, 2019.

- [75] *BAE Systems Delivers First Radiation Hardened RAD5545 Radios*, 2020 (accessed September 28, 2020). [Online]. Available: <https://www.baesystems.com/en/article/bae-systems-delivers-first-radiation-hardened-rad5545-radios>
- [76] L. P. Houssay, "Robotics and Radiation Hardening in the Nuclear Industry," Ph.D. dissertation, State University System of Florida, 2000.
- [77] P. Weber and C. Vanecek, "SIMON [Semi-Intelligent Mobile Observing Navigator] Combines Radiation Hardness with Computer Power," *Nuclear Engineering International*, vol. 35, no. 430, pp. 34–35, 1990.
- [78] "Making Tracks to Clean-Up after Accidents," *Nuclear Engineering International*, vol. 39, no. 476, p. 26, 1994.